

Control of Ignition Temperature in Hybrid Thermite-Intermetallic Reactive Systems

by

Christian Poupart

Thesis submitted to the
Faculty of Graduate and Postdoctoral Studies
In partial fulfillment of the requirements
For the M.A.Sc. degree in
Mechanical Engineering

Ottawa-Carleton Institute for Mechanical and Aerospace Engineering
Faculty of Engineering
University of Ottawa

© Christian Poupart, Ottawa, Canada, 2015

Abstract

Thermite compounds have received a renewed interest due to their ability to store large quantities of energy that is comparable to conventional energetic materials. Such reactive materials can be manipulated to create a nanolaminated structure. It has been shown that an increase in the fraction of nanolaminated particles can reduce the ignition temperature and increase reactivity. In the present study, methods to lower the ignition temperature of aluminium copper-oxide (Al-CuO) are assessed. Arrested reactive milling (ARM) was used on stoichiometric Al-CuO powders to increase the nanolamination and reduce the ignition temperature to 840 Kelvins (K). Milling alone not only reduced the ignition temperature slightly, but for milling times greater than 30 minutes, intermediate phases were produced, which had negative impacts on the reaction characteristics. Another method to reduce the ignition temperature of Al-CuO involved creating a hybrid mixture using a compound with a lower ignition temperature to further decrease the ignition temperature of Al-CuO. ARM was used to lower the ignition temperature of a nickel aluminium (Ni-Al) intermetallic compound down to 480 K. Hybrid mixtures were then created with varying concentrations of milled and unmilled Al-CuO-Ni. Powders were then tested in a tubular furnace to determine the ignition temperature dependence on heating rate and concentration of constituents. It has been shown that an unmilled hybrid mixture with 75% and 50% concentration of Al-CuO has an ignition temperature of 840 K. Higher concentrations of Ni-Al resulted in lowered ignition temperatures which varied between 600 K and 480 K. A milled hybrid mixture has lower ignition temperatures than an unmilled mixture. It was shown that a milled hybrid mixture with a 75% concentration of Al-CuO has an ignition temperature of 840 K, corresponding to pure Al-CuO. The ignition temperature of the milled hybrid mixture was reduced to approximately 520-620 K for concentrations of Ni-Al of 50%, and 473-573 K for concentrations of 75% Ni-Al.

Acknowledgements

I would like to thank my supervisor Dr. Matei Radulescu for his mentorship, guidance and serviceable feed-back throughout my years under his supervision. I would also like to thank Dr. Antoine Bacciochini for his expert insight and guidance during my time here at the University, Dr. Mohammed Yandouzi for allowing me to use the scanning electron microscope (SEM) and x-ray diffraction (XRD) machine. I would like to thank my colleagues Geoff Maines and Jonathan Armstrong for their tutorship with GnuPlot, data processing, and their help conducting experiments. I would also like to thank Dr. Sam Goroshin at the McGill University for his contribution to the experimental setup that was used to determine the ignition temperatures. Finally, I would like to thank the Canadian Space Agency (CSA) for their funding, making this research possible.

Table of Contents

List of Tables	vi
List of Figures	vii
1 Introduction	1
1.1 Background and Motivation	1
1.2 Literature Review	2
1.3 This Study	11
2 Experimental Procedure	12
2.1 Powders	12
2.2 Mechanical Alloying	13
2.3 Ignition	15
2.4 Flame Speed Measurements	19
3 Results and Discussion	21
3.1 Al-CuO	21
3.1.1 Morphology	21
3.1.2 Ignition Temperature	24
3.1.3 Flame Propagation	27

3.2	Ni-Al	29
3.2.1	Ignition Temperature	34
3.3	Hybrid Mixture - Hand mixed	37
3.3.1	Morphology	37
3.3.2	Ignition	37
3.4	Hybrid Mixture - Milled	41
3.4.1	Hybrid Mixture Procedure	41
3.4.2	Morphology	42
3.4.3	Ignition	43
4	Ignition Model	47
4.1	Single Phase System	48
4.1.1	Parameters	48
4.2	Two Phase Ignition Model	53
5	Further Discussions and Recommendations	58
5.1	Mechanical alloying	58
5.1.1	Al-CuO	58
5.1.2	Ni-Al	59
5.2	Hybrid System	60
6	Conclusion	61
	Appendices	62
	A Mathematica Code for Ignition Model	63
	References	64

List of Tables

1.1	Maximum milling time for Al-CuO as a function of added PCA (hexane), from Umbrajkar et al. [7]	5
2.1	Mechanical mill settings for Al-CuO and Ni-Al	14
4.1	Parameters used in the ignition model for individual mixtures of Al-CuO and Ni-Al	49

List of Figures

1.1	Maximum heat of reaction of Al-CuO, Ni-Al and conventional reactive materials from <i>webbook.nist.gov</i> , Fischer et al. [1]	2
1.2	Working principle behind high energy ball milling	4
1.3	60 minute milled Al-CuO mixtures using 8 ml of hexane, from Umbrajkar et al. [7]	6
1.4	Effects of particle size and milling time on the ignition temperature of Nickel Aluminium (<i>modified from Manukyan et al. 2012 [20]</i>)	8
1.5	Typical morphology (a), and cross-sectional microstructure (b) of milled Ni-Al powders from (<i>Bacciochini 2012</i>) [29]	10
2.1	Typical morphology of unmilled Al-CuO (a) and Ni-Al (b) prior to milling	13
2.2	Pictures of Planetary ball mill (2.2a), and Vials with Easy-GTM lids (2.2b) used to conduct mechanical alloying	14
2.3	Typical temperature (dashed line) and pressure (solid line) evolution given by Easy GTM lids during the milling operation for a Ni-Al mixture	15
2.4	Furnace schematic showing overview of components used to conduct ignition temperature experiments	16
2.5	Close up view of experimental furnace used to conduct ignition temperature experiments	16
2.6	Image of tubular furnace and experimental setup to determine ignition temperatures	17

2.7	Typical temperature (red) and voltage (blue) evolution with respect to time for a mixture of 16 minute milled Al-CuO	18
2.8	Steel channel for flame speed measurements	19
2.9	Steel channel inserted in insulating foam used to conduct flame propagation speed measurements	20
2.10	Schematic overview of experimental setup used to determine the flame speed of reactive powders	20
3.1	Unmilled mixture of Al-CuO demonstrating the morphology and particle size distribution	22
3.2	SEM images of milled Al-CuO stoichiometric mixtures for different mill times	23
3.3	X-Ray Diffraction results for mixtures of unmilled and milled Al-CuO powders	24
3.4	Typical temperature and voltage evolution with respect to time of heated 16 minute milled Al-CuO sample	25
3.5	Ignition temperature vs milling time for mixtures of milled Al-CuO	26
3.6	Ignition temperature vs heating rate for mixtures of milled Al-CuO	26
3.7	Reconstruction of flame propagation images for unmilled (a-f) and 16 minute milled powders (g-l) for Al-CuO mixtures demonstrating the flame front evolution as a function of time. From Maines et al. [30]	28
3.8	Average flame speeds related to milling time for Al-CuO	29
3.9	SEM image showing morphology and overall particle size of unmilled Ni-Al	30
3.10	SEM cross-sectional view of 16 minute milled Ni-Al	31
3.11	SEM cross-sectional view of 30 minute milled Ni-Al	31
3.12	SEM cross-sectional view of 40 minute milled Ni-Al	32
3.13	SEM image showing morphology and particle size of Ni-Al - 40 minutes milled	32
3.14	XRD study of unmilled and milled mixtures of Ni-Al powders	33

3.15	Temperature (red, orange) and voltage (blue) evolution with respect to time for 16 minute and 40 minute milled Ni-Al	34
3.16	Ignition temperatures vs mill time for mixtures of milled Ni-Al	36
3.17	Ignition temperatures vs heating rate for mixtures of milled Ni-Al	36
3.18	Typical morphology of hand mixed 50% 40 min Ni-Al and 50% 16 min Al-CuO hybrid mixture	38
3.19	Unmilled hybrid mixture ignition temperature plotted with respect to the added Ni-Al mass fraction	39
3.20	Unmilled hybrid mixture ignition temperature plotted with respect to the heating rate	40
3.21	Milled hybrid mixture procedure	41
3.22	Typical SEM cross-sectional view of a milled hybrid mixture	42
3.23	X-ray diffraction study results of a milled Al-CuO-Ni system at concentrations of 25%, 50%, and 75% added Ni-Al mass fraction	43
3.24	Temperature and voltage (blue) evolution for milled hybrid mixtures of Al-CuO-Ni at concentrations of 25, 50 and 75 percent of Ni-Al by mass	44
3.25	Milled hybrid mixture ignition temperature results for varying mass fractions of Ni-Al	45
3.26	Milled hybrid mixture ignition temperature plotted with respect to the heating rate	46
4.1	Ignition model for Al-CuO for varying values of pre-exponential factor Z	51
4.2	Temperature (blue) and concentration (red) evolution with time of Al-CuO from the ignition model	51
4.3	Ignition model for Ni-Al for varying values of pre-exponential factor Z	52
4.4	Temperature (blue) and concentration (red) evolution with time of Ni-Al from the ignition model	52

4.5	Typical temperature evolution for an ignition model of a hybrid system where the ignition temperature occurred at 873 K	55
4.6	Ignition model showing the temperature (blue) and concentration (red) evolution of a hybrid mixture with 22.15% added Ni-Al	55
4.7	Typical temperature evolution for an ignition model of a hybrid system where the ignition temperature occurred at 500 K	56
4.8	Experimental and theoretical temperature evolution with respect to the concentration of added Ni-Al in a hybrid system	57

Nomenclature

PCA	Process control agent
RPM	Rotations per minute
MIC	Metastable intermolecular composite
ARM	Arrested reactive milling
TMD	Theoretical maximum density
DSC	Differential scanning calorimetry
EDS	Energy dispersive spectroscopy
LCM	Lump capacitance method

Chapter 1

Introduction

1.1 Background and Motivation

Metal fuels such as Aluminium, Tantalum, Lithium, or Magnesium can be combined with metal oxides (CuO , Fe_2O_3 , MoO_3) to create highly reactive thermite mixtures. Thermite mixtures have received renewed interest in recent years due to their high energy density, high combustion temperature, and large gas production [1, 2, 3]. Thermite mixtures, or "Goldschmidt reactions" made a commercial appearance in the late 19th century [4]. A largely popular mixture was $\text{Al}+\text{Fe}_2\text{O}_3$ as this mixture had sufficient heat release to be used for railway track welding. Figure 1.1 shows that volumetric and specific heat of reaction can be larger in some thermite compounds when compared to conventional energetic materials such as PETN, TNT, and RDX. These energetics are extensively used in civilian and military applications [5, 6]. Thermite mixtures using aluminium as a metal fuel have seen increased popularity in recent years due to their high energy content, and the high availability of aluminium. High purity aluminium powder (> 98%) is readily available at a moderate price (*Alpha Aesar, Atlantic Engineer Equipment*) which makes these compounds attractive for scalability. This study focuses on the thermite mixture, aluminium copper-oxide (Al-CuO). Al-CuO is largely popular due to its ability to produce large quantities of gaseous products and a reaction front that can propagate at supersonic speeds. These traits make this compound attractive for many applications involving propellants, explosives,

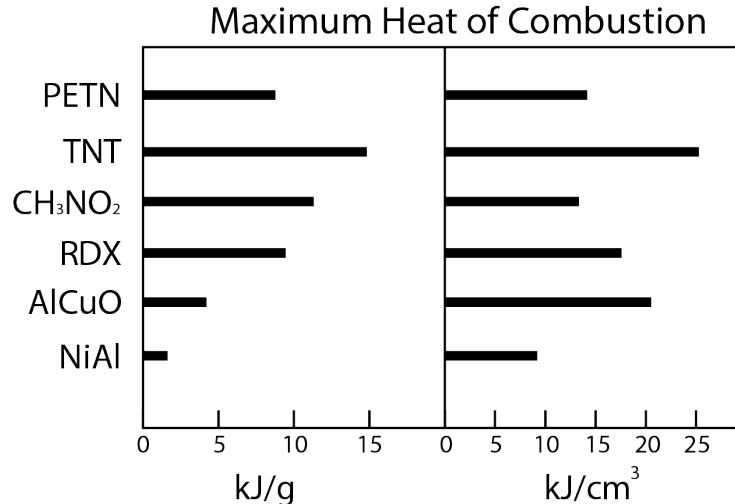


Figure 1.1: Maximum heat of reaction of Al-CuO, Ni-Al and conventional reactive materials from *webbook.nist.gov*, Fischer et al. [1]

and pyrotechnics. The ignition temperature of Al-CuO has been reported by Dreizin and Umbrajkar [3, 7] to be between 870-1273 K. Dreizin and Umbrajkar show that new technologies such as arrested reactive milling (ARM), or using nano-scale reactants may reduce the overall ignition temperature. Dreizin [3] explains that by manipulating the constituents interface, the reaction kinetics of these reactive materials may be improved. There is an interest in studying the ignition temperatures of such reactive materials to study gasless detonations [8], and heterogeneous flame propagation [9]. The goal of this study is to find a suitable method to decrease the ignition temperature of Al-CuO using a scalable, and relatively inexpensive method.

1.2 Literature Review

In recent years, methods to create reactive compounds with lower ignition temperatures have been explored. One method to lower the ignition temperature involves using nano-scale constituents to create mixtures known as MIC (metastable intermolecular composite). It was shown by Hunt et al.[10] that a decrease in particle size from the micron scale to nano scale can decrease the activation energy by one order of magnitude. The mixture studied was nickel-aluminium, an intermetallic compound which also uses aluminium as a

metal fuel. Cylindrical pellets of Ni-Al powders with 6.5 mm diameters were heated using a CO₂ laser. For an average aluminium particle size of 20 μ m, the activation energy was 162.5 kJ/mol, and for an average particle size of 40nm, the activation energy decreased to 17.4 kJ/mol. The activation energy strongly influences the ignition temperature of these reactive materials. It was shown that for reactive materials, a lowered activation energy leads to lower ignition temperatures [11].

Decreasing reactant particle size seems to be a strong lead in exploring methods to decrease ignition temperatures. Multiple methods of manufacturing nano-scale reactants were studied such as electro-exploded wires [12], flame synthesis [13], and wet chemistry [14]. These methods offer a solution for small-scale operations however, their low-production rate limits the scalability for commercial applications. Another disadvantage associated with creating nano-scale constituents is the poor surface contact between constituents, since the particles created usually have a spherical geometry. Dreizin [3] has concluded that the most cost-effective, and scalable method to decrease particle size while having a high surfact contact between constituents is the *arrested reactive milling* (ARM) technique. This method is considered a top-down approach, where micron sized particles are mechanically alloyed into smaller nano-scale particles.

ARM can be carried out using different ball mills such as vibratory mill, attritor mill, planetary mill, or horizontal ball mill. The working principle behind these types of ball mills remains the same [15]. Figure 1.2 shows the working principle behind high energy ball milling. Centrifugal forces acting on spherical steel balls are transferred to the mixture of powders, subsequently crushing them together. Mechanical milling is used to reduce micron-sized particles down to sub-micron level and promote intermixing. In principle, this solid state process allows particulates to be cold welded together creating more refined micro-structures, better homogeneity, and better surface contact between constituents [16, 17]. Reactive powder mixtures are created using specific settings (i.e. ball to powder mass ratio, amount of process control agent (PCA), milling duration), and are milled until mechanical activation occurs during the milling process. Identical mixtures are milled using the same settings, but the process is stopped before mechanical activation occurs,

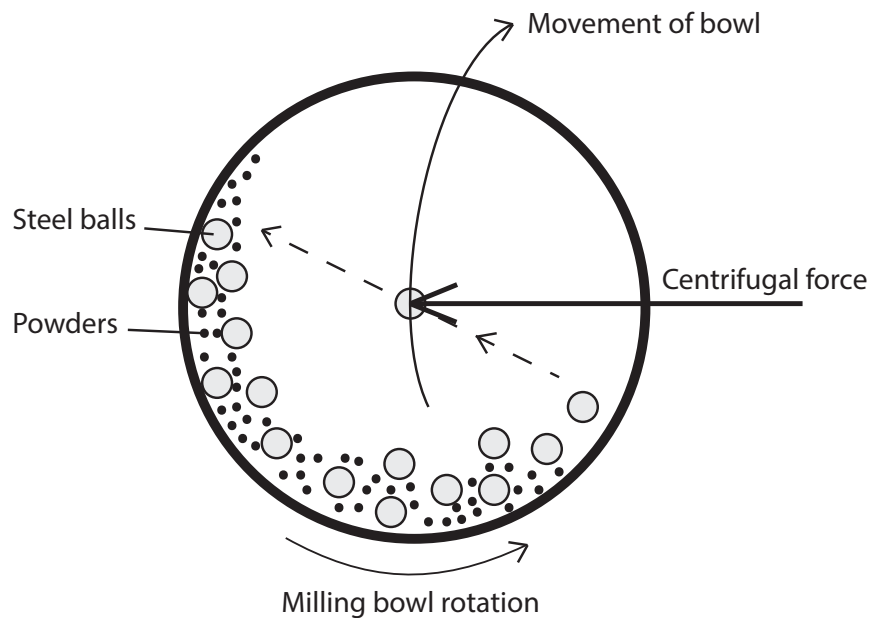


Figure 1.2: Working principle behind high energy ball milling

hence the name arrested reactive milling. The addition of a PCA allows for longer periods of milling, inhibits local reaction of reactants and prevents cold welding of powders on the walls of the vials [18, 7]. A typical PCA which is widely used in literature is Hexane, which is attractive due to its ability to evaporate easily, therefore powders can be easily extracted [7, 19, 20, 21, 22].

A study by Umbrajkar et al. [7] investigated the effects of arrested reactive milling on stoichiometric mixtures of Al-CuO. Dry milling and wet grinding using hexane as a PCA were performed as two methods of high energy ball milling. Umbrajkar showed that using hexane as a PCA yielded smaller particle size, thus increasing surface to volume contact ratio and improving reaction kinetics. They also showed that by using a PCA, the maximum milling time could be increased, further reducing particle size. Lower ignition temperatures for Al-CuO mixtures have been reported by Umbrajkar et al.[7] when using the ARM method. Maximum milling time from their study are shown in table 1.1, for varying amounts of hexane. Stoichiometric mixtures of Al-CuO were initially milled until mechanical activation occurred. When dry milling was performed, the reaction time was 2 minutes. Adding 1 ml of hexane yielded a maximum milling time of 16 minutes, and adding 8 ml of hexane yielded no reaction after 60 minutes of milling. Figure 1.3 shows

Hexane (ml)	Maximum milling time (min)
0	2
1	16
8	60

Table 1.1: Maximum milling time for Al-CuO as a function of added PCA (hexane), from Umbrajkar et al. [7]

a cross-sectional view of the micro-structure of 60 minute milled Al-CuO powders. The overall particle size remained in the order of 1-30 microns however, the constituent interface was reduced to a nano-scale. By using the ARM method the copper-oxide particles became embedded in the aluminium matrix, yielding a much better surface contact ratio between constituents when compared to mixing nano particles of reactants. Powders were then heated on electrically heated Nichrome wire in order to determine the ignition temperatures. Results for a 16 minute milled mixture of Al-CuO with 1 ml of hexane yielded average ignition temperatures of 890 K. A 60 minute milled system with 8 ml of hexane reacted at approximately 650 K for heating rates between 10^4 and 10^5 Kelvins per minute. X-ray diffraction (XRD) analysis showed that local reactions had started forming during the milling operation for a 60 minute milling time. The additional products took the form of CuAl_2 , Cu_2O , Cu_9Al_4 , Al_2O_3 and pure Cu.

Al-MoO₃ is another example of an aluminium-based thermite mixture. Granier et al.[23] found that Al-MoO₃ mixtures with micron scale particles react at approximately 880 K. The effects of ARM on Al-MoO₃ was studied by Umbrajkar et al.[18]. Mixtures were milled for 60 minutes using a shaker mill. A total of 5 grams of powders was added to each vial, with a ball-to-powder mass ratio of 5 using spherical steel balls. Powders were ignited using an electrically heated wire at heating rates ranging from 10^4 to 10^6 K/s. Results showed that by milling Al-MoO₃, ignition temperatures could be reduced from 880 K down to approximately 675 K.

The ARM method seems suitable in decreasing the ignition temperature of reactive materials such as Al-CuO, however the introduction of intermediate phases have negative

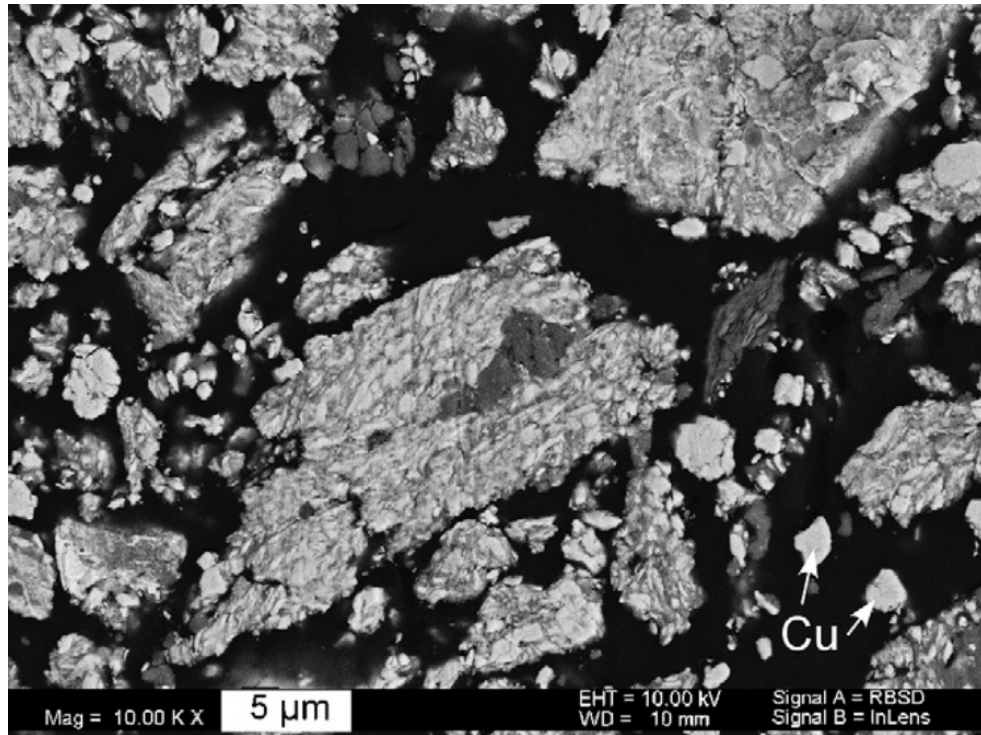


Figure 1.3: 60 minute milled Al-CuO mixtures using 8 ml of hexane, from Umbrajkar et al. [7]

impacts on the exothermicity of reactive materials, and are undesirable. Another method to lower the overall ignition temperature of Al-CuO has been explored by Ilunga [24]. In their study a hybrid Al-CuO-Si-Bi₂O₃ mixture was created, for which the lowest ignition temperature obtained was 886 K. The objective of this method was to lower the ignition temperature by introducing a reactive compound that has a lower ignition temperature, to the Al-CuO mixture.

There are many reactive mixtures that exist in the literature that could be used to create such hybrid mixtures [1]. However, information about the ignition temperature of mechanically alloyed mixtures remains limited. Shoshin et al.[25] studied the effects of milling aluminium rich mixtures of Ti-Al. They found that for mixtures of 75% Al, the ignition temperatures varied around 900 K. Schoenitz et al.[26] studied the effects of mechanical milling on the ignition temperatures of mixtures of Al-MoO₃, Al-Fe₂O₃, and B-Ti. They found that at a heating rate of 340 K/min, milled Al-MoO₃ reacted at 995 K. Milled Al-Fe₂O₃ reacted at 1110 K for heating rates of 291 K/min. Finally, milled mixtures of B-Ti reacted at 600 K for heating rates of 412 K/min. These mixtures were deemed unsuitable candidates for creating a hybrid mixture because the ignition temperatures were too high.

Motlagh et al. (2012) [27] investigated the effects of milling an aluminium rich Al-CuO-Ni system in order to produce a welding agent. The hybrid mixture was milled using 4 ml of hexane as a PCA. Initial particle sizes were less than 100 μ m for Al and less than 20 μ m for Ni. A result of this study was a decrease in ignition temperature of the hybrid system. A milling period of 5 hours yielded ignition results of approximately 550 K. The addition of Ni-Al intermetallic showed promising results, and this intermetallic mixture was further investigated.

Manukyan et al. [20] have shown the ignition temperature of unmilled Ni-Al to be 913 K. Hunt et al. [10] saw that at heating rates of 0.5 K/min unmilled stoichiometric Ni-Al reacted at 825 K, and at heating rates of 40 K/min Ni-Al reacted at 890 K. Studies have shown that high energy ball milling has an important effect on the ignition temperature of Ni-Al intermetallic mixture and can yield ignition temperatures as low as 500-530 K

[20, 28]. Manukyan et al.[20] analysed the influence of sequence and duration of mechanical milling on the microstructure and ignition temperature of Ni-Al systems. Initial particle size of aluminium and nickel were $45\mu\text{m}$ and $5\mu\text{m}$ respectively. Mixtures of stoichiometric Ni-Al powders were processed in a planetary ball mill at a ball to powder mass ratio of 5:1 for different milling times. Milling speeds were set to 650 rpm. Both dry milling and wet grinding with hexane were performed. Results are shown in figure 1.4. In figure

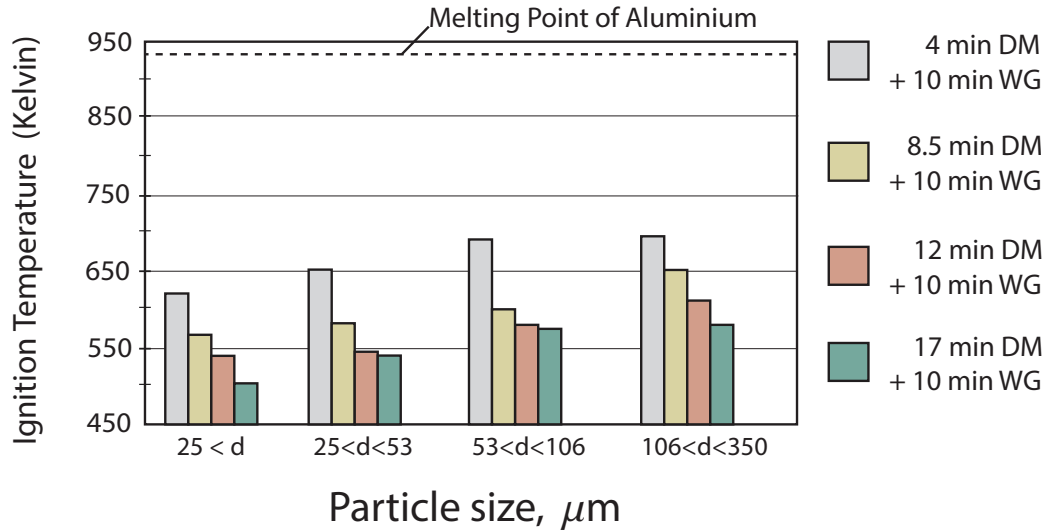


Figure 1.4: Effects of particle size and milling time on the ignition temperature of Nickel Aluminium (*modified from Manukyan et al. 2012 [20]*)

1.4, DM refers to Dry Milling, and WG refers to Wet Grinding. Dry milling resulted in maximum milling times of 17.5 minutes. After the dry milling process, 10 minutes of WG was performed, for all samples. The use of a process control agent allowed powders to be milled for an additional period of time, thus further decreasing particle surface to volume ratio, increasing the surface contact of constituents, and lowering the ignition temperature. Figure 1.4 shows the importance of milling time on the ignition temperature of such a system.

Mukasyan et al.[28] showed that a reduction in particle size has an important effect on the ignition temperature. Ni-Al particle sizes previous to mechanical activation were $40\mu\text{m}$ and $5\mu\text{m}$. Powders were milled with a ball-to-powder mass ratio of 10:1 for 5 minutes using a planetary ball mill. Milling was performed in an argon environment, and no PCA was

used. Compacted cylindrical pellets with 75-85% TMD were created using the mechanically milled powders. These pellets were tested in a furnace equipped with time-resolved XRD. Heating rates varied between 5 and 100 K/min. Results showed that mechanical alloying reduced the ignition temperature down to 680 K for 40 μ m reactants and 540 K for 5 μ m reactants.

In a study parallel to this thesis, Bacciochini et al.(2012)[29] demonstrated the effects of mechanical milling on the microstructure of mixtures of Ni-Al. Initial average particle size of aluminium was 4.2 microns, and 6.8 microns for nickel. Settings used by Bacciochini were; 600 rpm bowl rotational speeds, a ball-to-powder mass ratio of 20:1, and 42 minutes maximum mill time. Mechanical alloying resulted in a compound with a refined microstructure with constituents intermixed on a nano-scale. Figure 1.5(b) show elongated lamelas of nickel (light gray) embedded in the aluminium matrix (dark grey). These lamelas vary in width averaging around 670 nano-meters. Mill settings used by Bacciochini et al.[29] greatly influenced the settings used for this study.

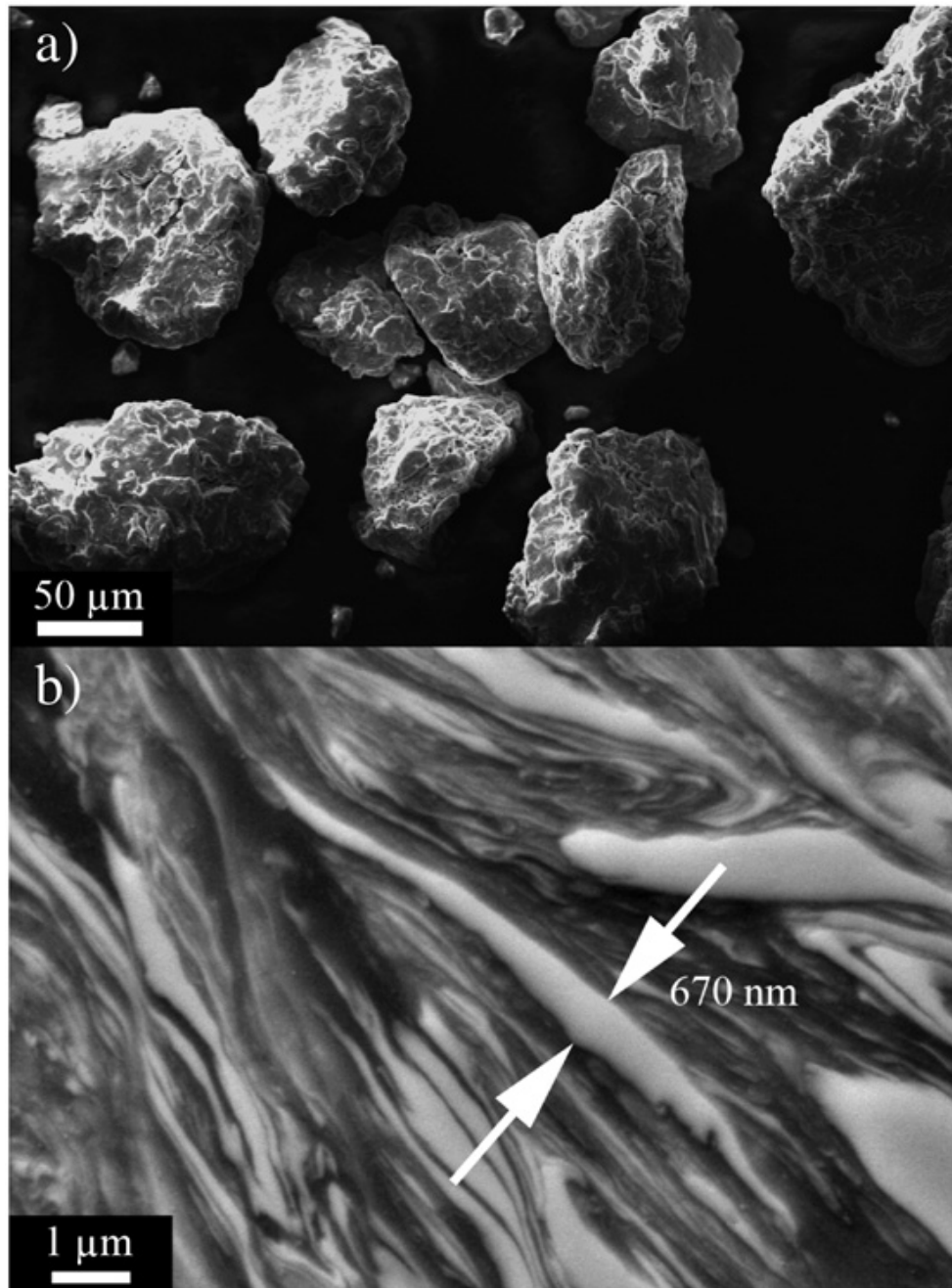


Figure 1.5: Typical morphology (a), and cross-sectional microstructure (b) of milled Ni-Al powders from (*Bacciochini 2012*) [29]

1.3 This Study

The review in section 1.2 showed that there are two methods to decrease the ignition temperature of Al-CuO. The first method is to produce nano-sized constituents to create the reactive mixture. As was shown by Hunt et al. [10], a decrease in particle size of aluminium lead to lower activation energies. A promising method to create nano-scale constituents is the arrested reactive milling technique. Umbrajkar et al.[7] showed that ARM yields smaller particle size, more refined micro-structures, and lower ignition temperatures for Al-CuO. The second method to lower the ignition temperature of Al-CuO is to create a hybrid mixture using a constituent with lower ignition temperatures.

In this thesis we will consider both methods. We first consider the milling of Al-CuO alone and we monitor the formation of products, and how they affect the exothermicity of the mixture. The second part of this thesis focuses on creating a hybrid mixture with lower ignition temperatures. Ni-Al seems to be a suitable additive to further decrease the ignition temperature because it is sufficiently energetic [1], and once milled, it has low ignition temperatures [20]. Ni-Al is milled individually in order to capture the ignition behaviour as a function of milling time. Finally, we study the ignition characteristics of unmilled and milled hybrid mixtures of Al-CuO-Ni at varying Ni-Al mass fractions.

In this thesis we review the experimental procedure in chapter 2. In chapter 3 we provide experimental results and discussion. Chapter 4 shows our development for an ignition model. Chapter 5 covers our recommendations for future studies attempting to reduce the ignition temperature of Al-CuO. Finally, we conclude this thesis by going over our findings in chapter 6.

Chapter 2

Experimental Procedure

2.1 Powders

The aluminium powder used was 99.9% pure, 325 mesh (*Atlantic Engineer Equipment*), sifted to obtain particles of less than $25\mu\text{m}$. Copper-Oxide powder was also 99.9% pure, $1\text{-}5\mu\text{m}$ (*Alpha Aesar*), and Nickel powder was 99.9% pure with particle size averaging $7\mu\text{m}$ (*Atlantic Engineer Equipment*). Mixtures of Al-CuO and Ni-Al were made at stoichiometry. A 2:3 molar ratio for Al-CuO was created and a 1:1 molar ratio of Ni-Al was created to satisfy the following equations.



Compounds of Al-CuO and Ni-Al were first mixed by hand, followed by the mechanical milling process. In order to analyze the micro-structure of compounds, scanning electron microscopy (SEM) was performed using a *Zeiss, model Evo10* equipped with backscattered electron mode (BSE), energy dispersive spectroscopy (EDS) probe (INCA-x-act, Oxford Instruments, UK), electron backscatter diffraction (EBSD) and CT scan detectors. X-ray diffraction (XRD) with a *Philips X-Pert model PW 1830* with $\text{CuK}\alpha$ radiation allowed for monitoring the micro-structure and characterizing the phases of milled materials. The morphologies of the raw powders prior to milling are shown in figure 2.1.

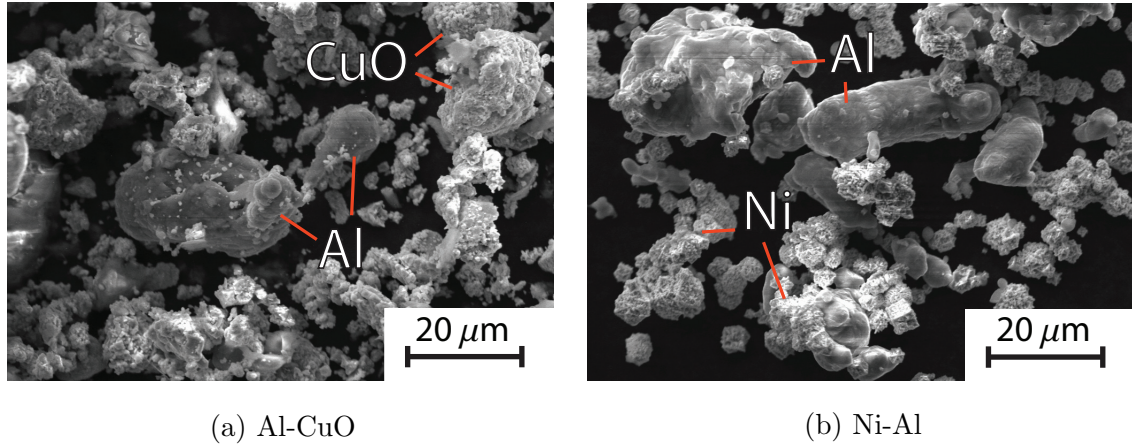


Figure 2.1: Typical morphology of unmilled Al-CuO (a) and Ni-Al (b) prior to milling

2.2 Mechanical Alloying

To achieve a nano-scale powder interface, powders were mechanically milled using a *Pulverisette 7* planetary ball mill as shown in figure 2.2a. A procedure similar to Umbrajkar et al (2006) [7], and Bacciochini et al. [29] was used. Mechanical milling was conducted in an Argon environment in order to inhibit oxidation of constituents. Powders and vials were placed in a *Labonco Precise Controlled Atmosphere* glovebox. In this study, 4 ml of Hexane was added while powder and vials were still in an argon environment. A total of 3.7 grams of stoichiometric powders was placed in each 80 ml hardened steel cups. The two vials were then sealed, removed from the glovebox, and placed in the ball mill. Mill settings are shown in table 2.1. The rotational speed was set at 450 rpm for Al-CuO, and 500 rpm for Ni-Al. A ball to powder mass ratio of 20:1 similar to Bacciochini et al. [29] was used to determine the quantity of added steel balls. Each vial was sealed with a *Fritsch Easy-GTM* lids, shown in figure 2.2b. The Easy GTM lids are equipped with a thermo-couple and a pressure sensor which allowed the ability to determine if mechanical activation occurred during the milling process.

A typical temperature and pressure evolution plot of a milling operation is shown in figure 2.3. The friction of powder and steel balls causes the increase of temperature and pressure, giving this plot an increasing trend with respect to time. An abrupt increase in pressure and temperature characterizes a mechanical activation event. This specific



(a)

(b)

Figure 2.2: Pictures of Planetary ball mill (2.2a), and Vials with Easy-GTM lids (2.2b) used to conduct mechanical alloying

Table 2.1: Mechanical mill settings for Al-CuO and Ni-Al

Mixture	Ni-Al	Al-CuO
Mass (g)	3.7	3.7
RPM	500	450
Total mill time (min)	8, 16, 30, 40	16, 30, 46, 60, 120
Hexane (ml)	4	4

temperature-pressure evolution in figure 2.3 shows a case where mechanical activation has occurred for Ni-Al. In order to prevent damage on the Easy GTM lid sensors custom steel lids shown in figure 2.2b were used for the cleaning process. Milling times were determined by milling the reactants under the conditions described in table 2.1 until mechanical activation occurred. Mechanical activation is characterized by an increase in temperature coupled with a spike in pressure recorded by the pressure sensor. Individual mixtures of Al-CuO and Ni-Al were milled separately until mechanical activation occurred during the milling process. By doing so, the maximum milling time for each compound was set.

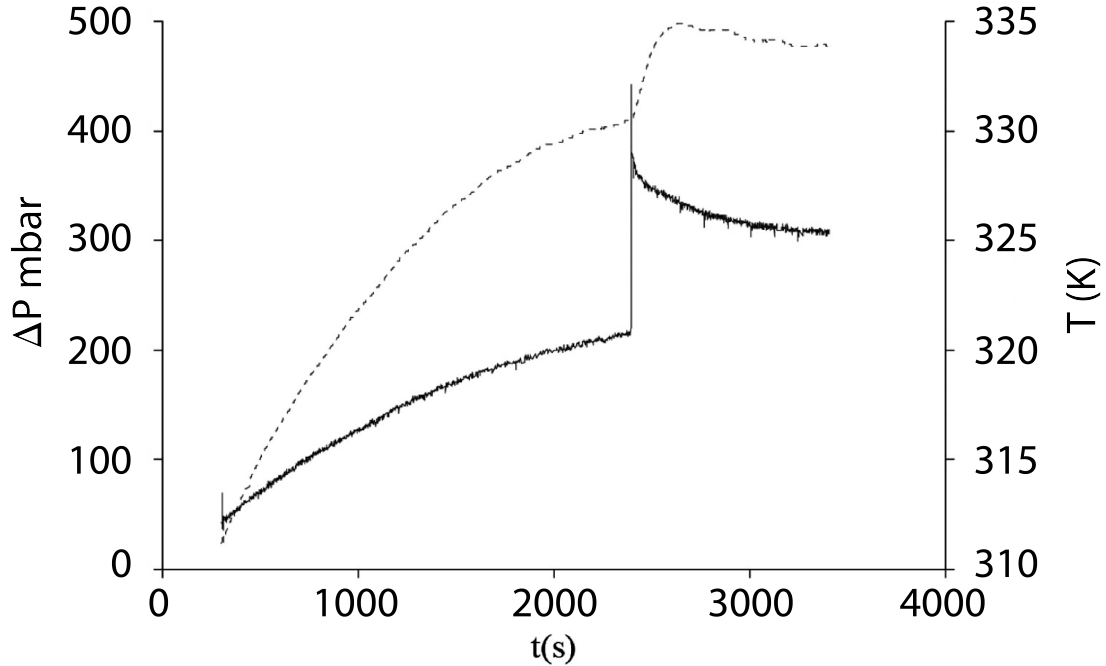


Figure 2.3: Typical temperature (dashed line) and pressure (solid line) evolution given by Easy GTM lids during the milling operation for a Ni-Al mixture

2.3 Ignition

Ignition temperatures were determined using the experimental setup shown in figures 2.4, 2.5, and 2.6. Milled powders were compacted into 3 mm diameter by 3 mm in height cylindrical pellets. Pellets had average densities of 3.24 g/cm³ and 3.47 g/cm³ yielding on average 65% TMD for Al-CuO and Ni-Al respectively. The theoretical maximum density (TMD) was calculated using equation (2.3).

$$TMD = \frac{M_{tot}}{V_{tot}} = \frac{nW_1 + nW_2}{\frac{nW_1}{\rho_1} + \frac{nW_2}{\rho_2}} \quad (2.3)$$

Where n is the mole fraction, W_i is the molecular mass of the compound, and ρ_i is the respective density. A *Watlow* 60 Volts tubular furnace was used to heat the samples. The furnace was heated at different heating rates between (30-100 K/min) until ignition. Figure 2.4 shows an overall view of the experimental setup that was used to determine the ignition temperatures of the compounds. Figure 2.5 shows a more detailed view of the furnace, showing the focusing lens used to focus the photodiode onto the pellet. Figure

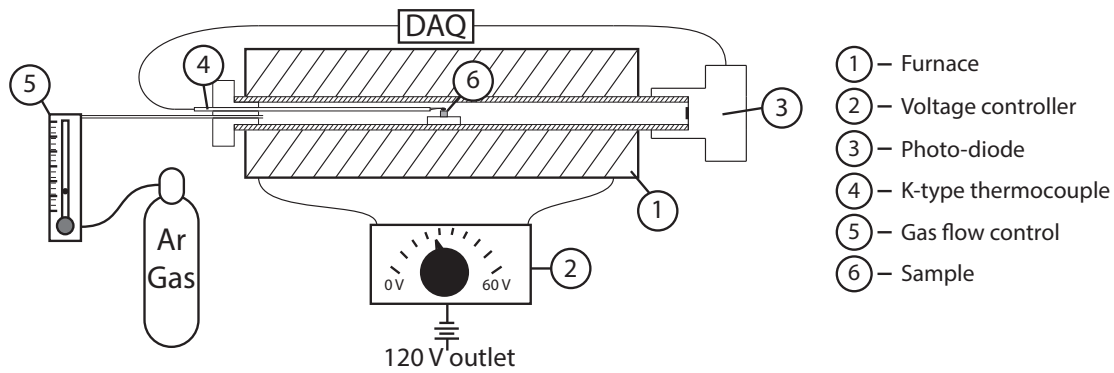


Figure 2.4: Furnace schematic showing overview of components used to conduct ignition temperature experiments

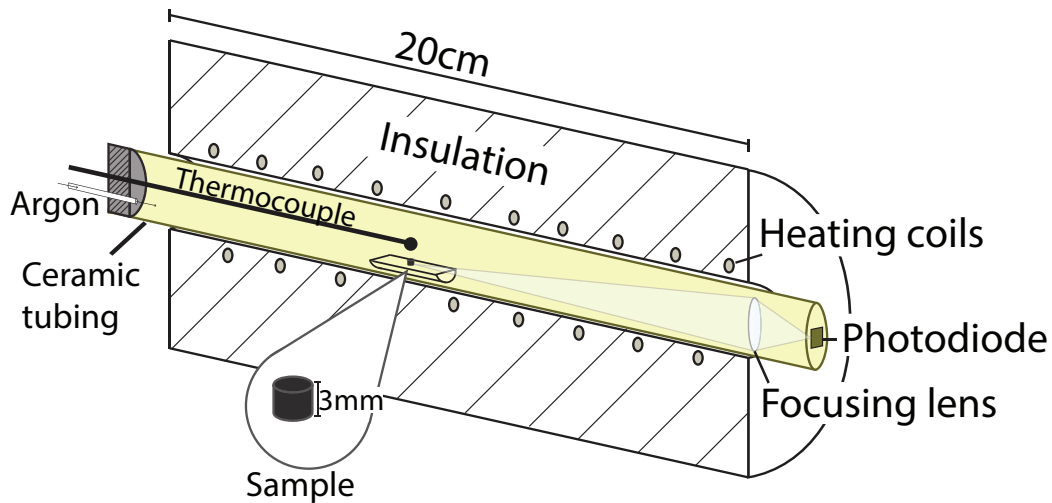


Figure 2.5: Close up view of experimental furnace used to conduct ignition temperature experiments

2.6 shows an image of the experimental setup. A micro flow of argon was passed through the furnace in order to prevent oxidation of samples during heating. Once the pellet was formed, it was placed on a half-cylindrical ceramic piece. This piece was then pushed through the ceramic tube. Once at a specific position, the end pieces were placed (argon flow, thermocouple and photo-diode) allowing for an atmospheric seal of the apparatus. The Argon flow was then fed through the inlet on the left hand side of figure 2.5. Five minutes was allowed to pass in order to allow sufficient argon to fill the chamber, and this flow was kept on during heating of samples. The heating rates varied between 30 and 100 K/min. A 1/8" K-type thermo-couple probe from *Omega Engineering* measured

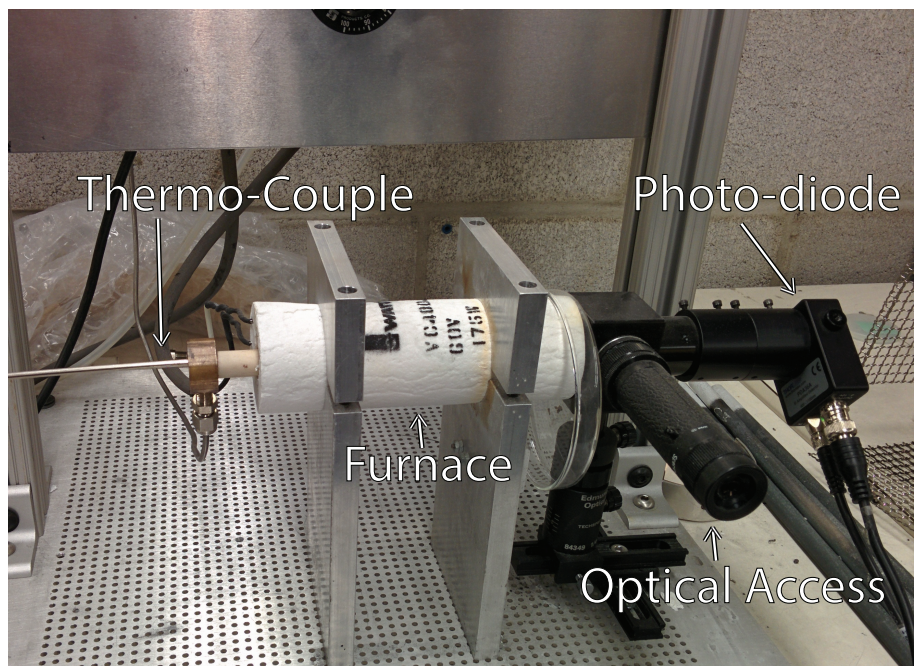


Figure 2.6: Image of tubular furnace and experimental setup to determine ignition temperatures

the temperature evolution directly above the sample shown in figure 2.5 and 2.6. Since the heating rates were relatively low, the temperature is assumed to be uniform in the furnace, as well as in the sample. A photo-diode was placed at the end, and a focusing lens aimed directly at the heating sample. Powders were heated until the ignition event was captured. Once ignition occurred, a plot similar to figure 2.7 was obtained using a National Instruments data acquisition system (PXIe-1073 hub with PXIe-6358 card) connected to a computer. Figure 2.7 shows the temperature evolution given by the thermocouple, as well as the voltage evolution given by the photo-diode. The red line represents the temperature evolution given by the K-type thermocouple. The slope of the temperature curve gave us the heating rate. The blue line represents the voltage emitted by the photo-diode. The spike in temperature coinciding with the large increase of luminescence characterizes the ignition event.

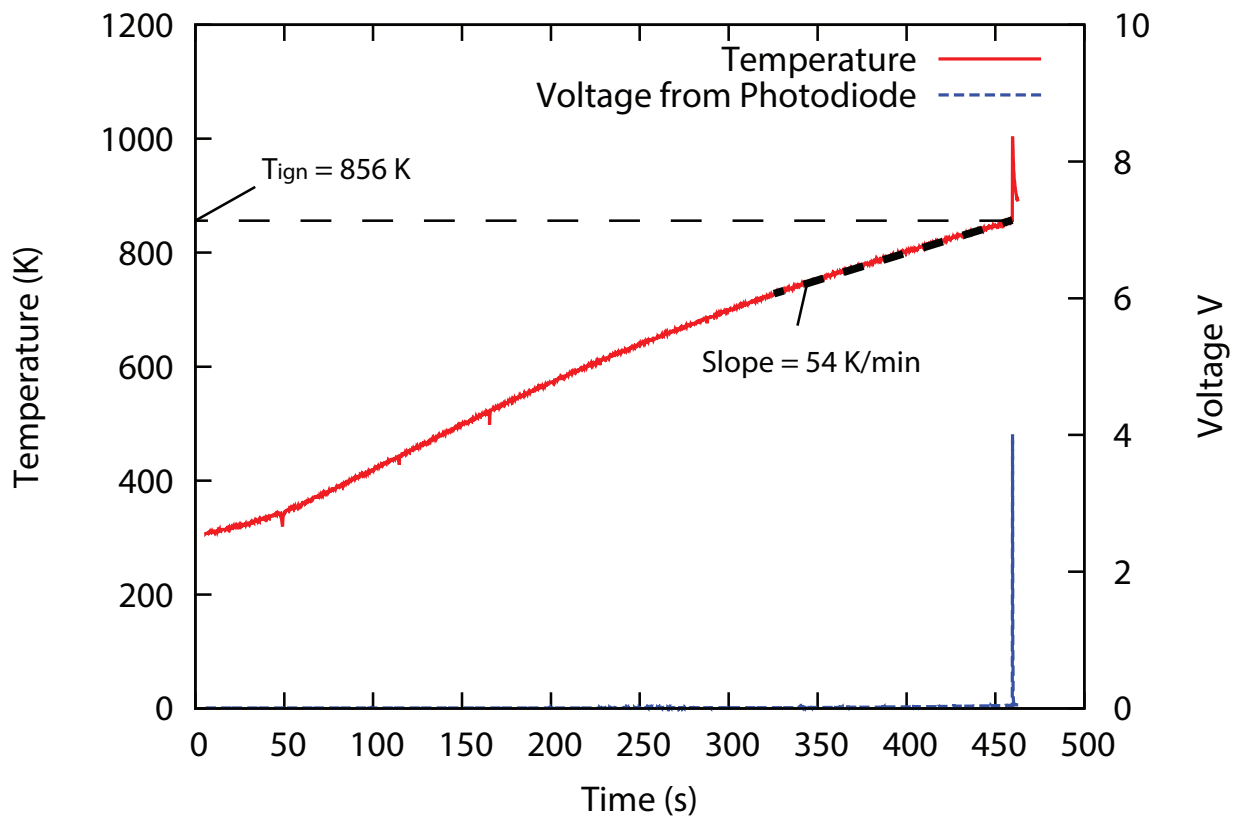


Figure 2.7: Typical temperature (red) and voltage (blue) evolution with respect to time for a mixture of 16 minute milled Al-CuO

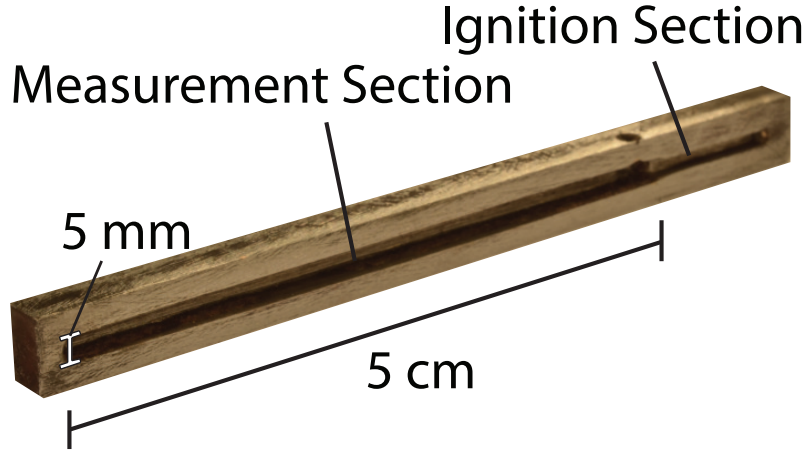


Figure 2.8: Steel channel for flame speed measurements

2.4 Flame Speed Measurements

An experimental setup was made to conduct flame speed measurements. These tests were made for a parallel study by Maines et al. [30]. Flame speeds were measured for milled and unmilled mixtures of Al-CuO. 530 ± 69 grams of powders were loosely packed to approximately 25% TMD in the measurement section of the channel shown in figure 2.8. The filled channel was then placed in a foam holder shown in figure 2.9. The microscope slide prevented gases from escaping and obstructing the view of the burning powders. Samples were lit in the ignition section of figure 2.8 using a butane torch. A mirror placed at 45° enables a high speed camera to view the ignition event without damaging the lens. A Phantom V1210 high-speed camera was used to capture the combustion of powders. Capture speeds varied between 6,000-20,000 frames per second depending on the sample. Aperture was set to f/2.8. Figure 2.10 shows the setup that was used to capture the flame propagation of Al-CuO.

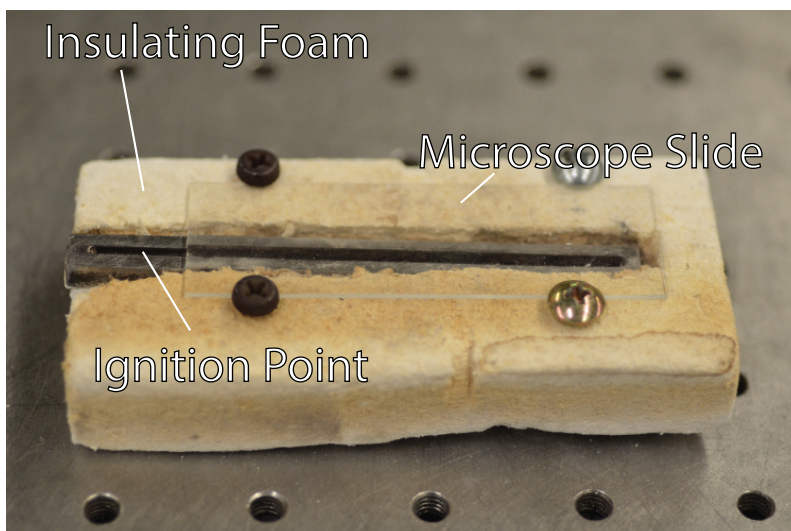


Figure 2.9: Steel channel inserted in insulating foam used to conduct flame propagation speed measurements

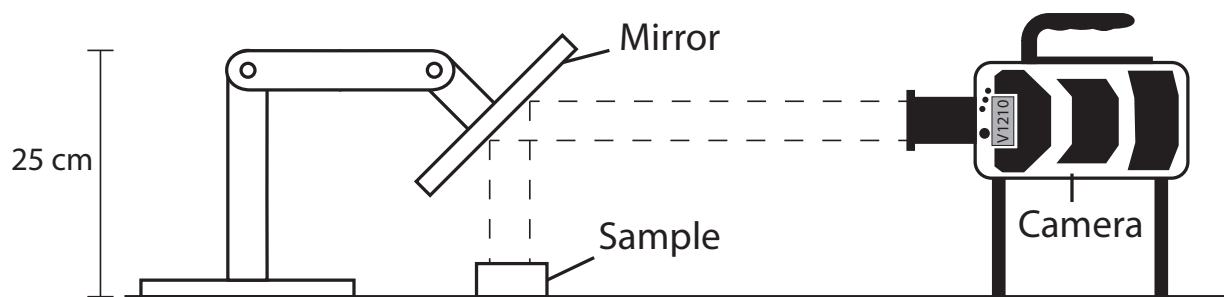


Figure 2.10: Schematic overview of experimental setup used to determine the flame speed of reactive powders

Chapter 3

Results and Discussion

3.1 Al-CuO

3.1.1 Morphology

An SEM image of unmilled stoichiometric Al-CuO is shown in figure 3.1. Initial particle size of unmilled powders varied between 1-5 microns for CuO, and 1-25 microns for Al. The darker particles represent aluminium, and the lighter grey particles represent copper-oxide.

Stoichiometric Al-CuO was milled using settings described in chapter 2. Mixtures were milled at different intervals from 16 minutes to 2 hours. Figure 3.2 depicts the morphology of milled powders for different milling times. A 16 minute milled mixture has particle size varying between 1-20 microns, which is approximately the starting particle size. Longer periods of milling yielded smaller overall particle size. A 60 minute milled mixture had particle size of 5 microns and less. The interface between constituents was reduced to a nano-scale. Particulates of CuO have become embedded in the aluminium matrix resulting in a more refined micro-structure with optimal surface contact to volume ratio. The ARM method proved to be a suitable method to decrease particle size, and promote intermixing of Al-CuO mixtures.

X-ray diffraction was performed on the samples of unmilled and milled mixtures of Al-CuO. Results are shown in figure 3.3. XRD results shown in figure 3.3 show that the

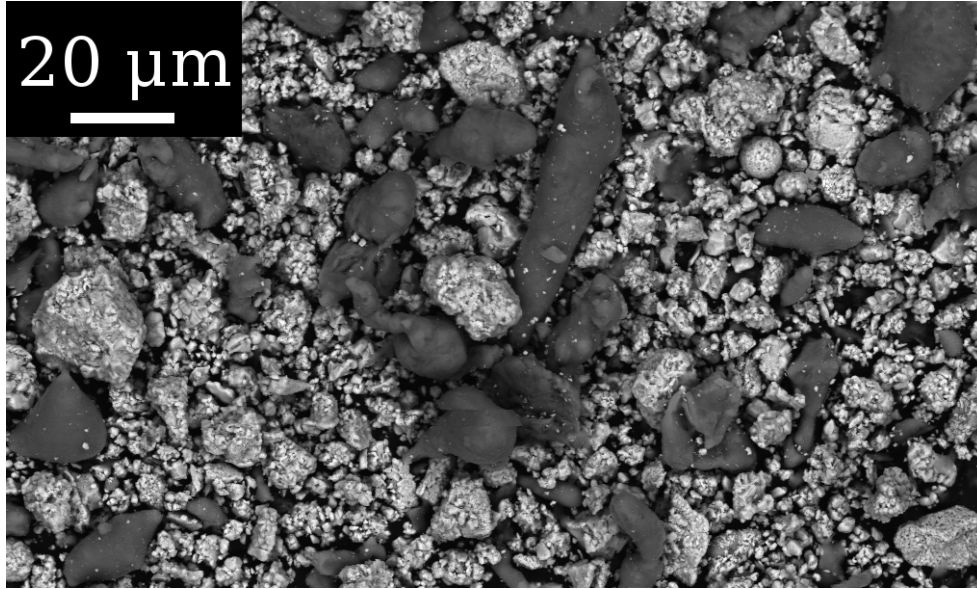


Figure 3.1: Unmilled mixture of Al-CuO demonstrating the morphology and particle size distribution

phase concentration of a 16 minute milled Al-CuO sample remains identical to that of unmilled powders. Milling times greater than 30 minutes resulted in the formation of intermediate phases, as a result of mechanical activation. These phases took the form of Cu , Al_2Cu , Al_2CuO_4 , Cu_2O , $AlCu$. The formation of secondary phases occurring while milling for longer periods of time are consistent to what Umbrajkar et al. [7] had found. Their results showed secondary phase formation for 60 minutes of milling, however nothing was reported for 30 and 46 minutes of milling. Complete reaction of Al-CuO during the milling process might have been inhibited by the process control agent, hexane. In a parallel study by Maines et al. [30], results have shown that exothermicity was reduced due to the formation of these intermediate phases. In accordance to the objectives stated in section 1.3, the maximum milling time for Al-CuO using the mill settings described in section 2, is 16 minutes.

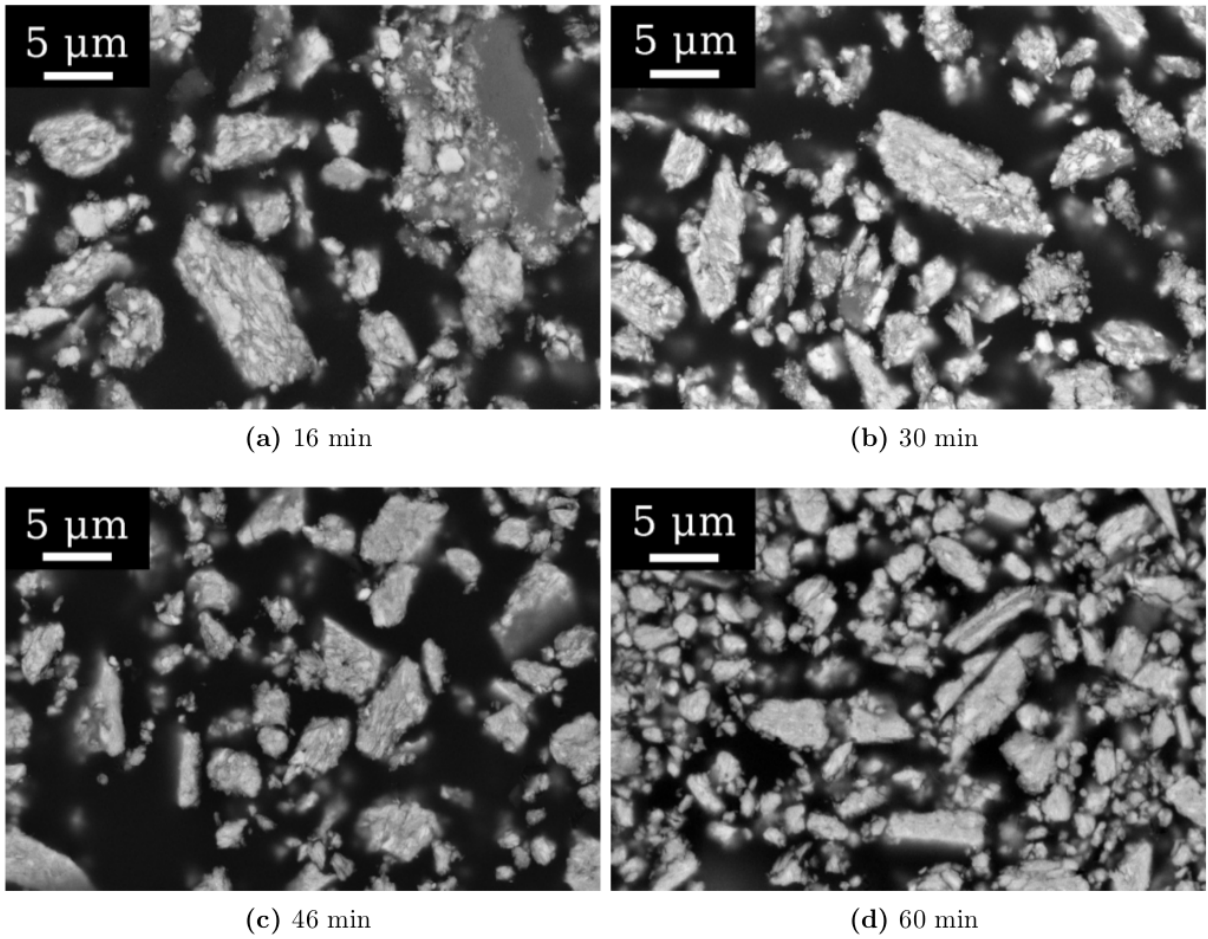


Figure 3.2: SEM images of milled Al-CuO stoichiometric mixtures for different mill times

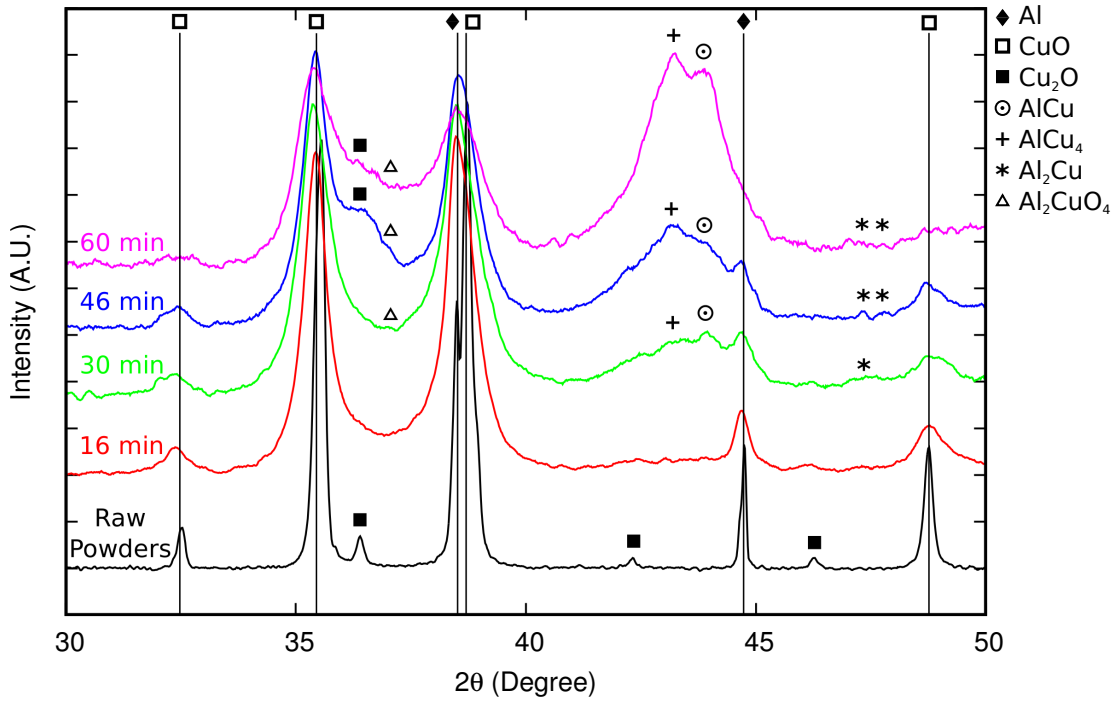


Figure 3.3: X-Ray Diffraction results for mixtures of unmilled and milled Al-CuO powders

3.1.2 Ignition Temperature

Compacted pellets described in section 2.3 were placed in the apparatus shown in figure 2.5 in order to determine the ignition temperature. The furnace was heated at different heating rates varying from 30 to 100 Kelvins per minute. Figure 3.4 shows a typical plot for the temperature and voltage evolution for a heated Al-CuO pellet. Results for the ignition temperature were plotted as a function of milling time (figure 3.5), and heating rate (figure 3.6).

Results in figure 3.5 confirm that the ignition temperature of thermites can be modified using the ARM technique. The 16 minute milled sample showed ignition temperatures varying around 873 K with a certain consistency. These results are consistent with Umbrajkar's results [7]. For mill times of 30 and 46 minutes, a transition is observed where the ignition temperature was either 873 K or approximately 420 K. Intermediate phases formed during milling believed to be responsible for the decrease in the ignition temperature since their appearance coincides with the transition phase to lower ignition temperatures. Milling times greater than 1 hour resulted in ignition temperatures of 420 K. Umbrajkar's results

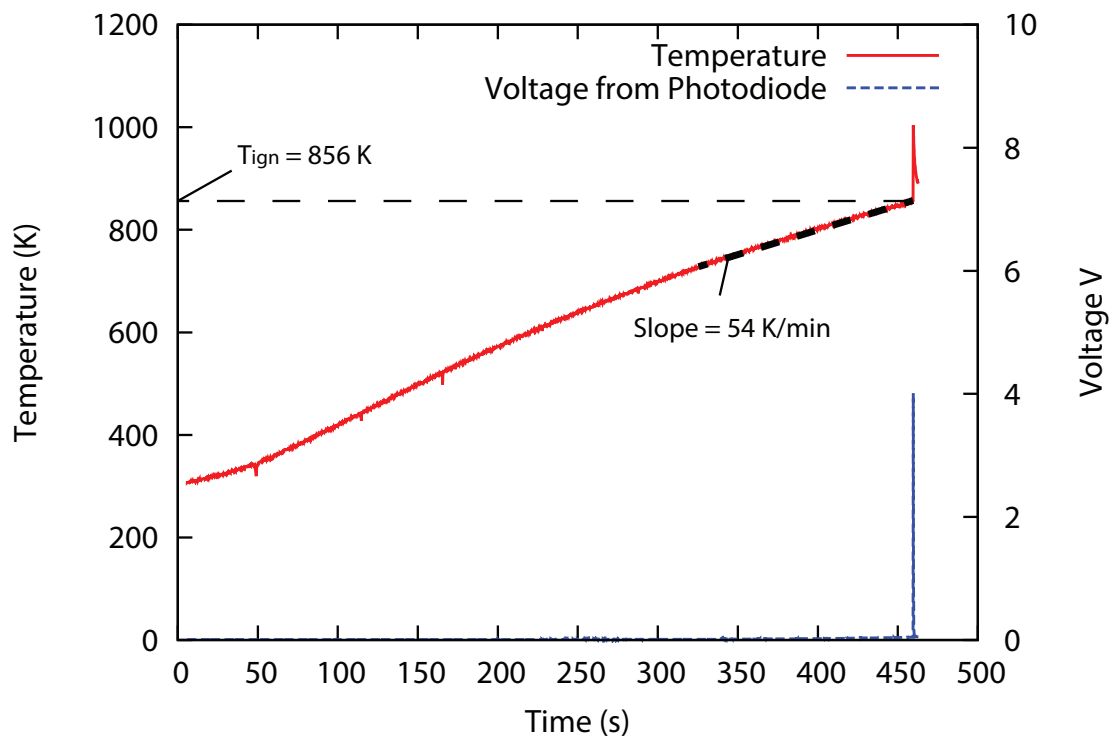


Figure 3.4: Typical temperature and voltage evolution with respect to time of heated 16 minute milled Al-CuO sample

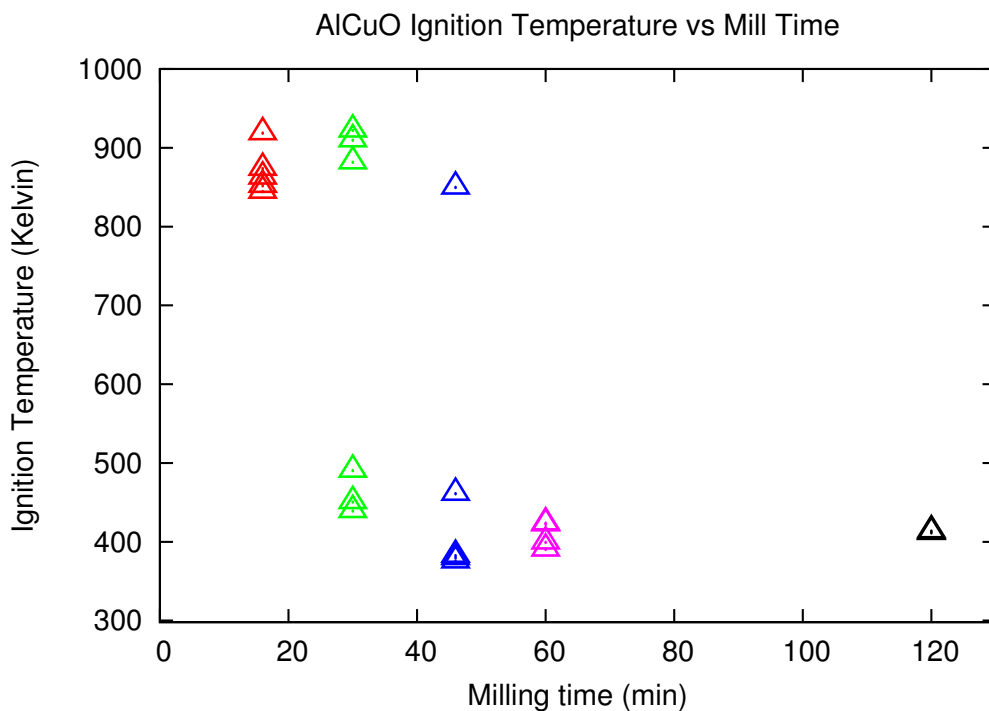


Figure 3.5: Ignition temperature vs milling time for mixtures of milled Al-CuO

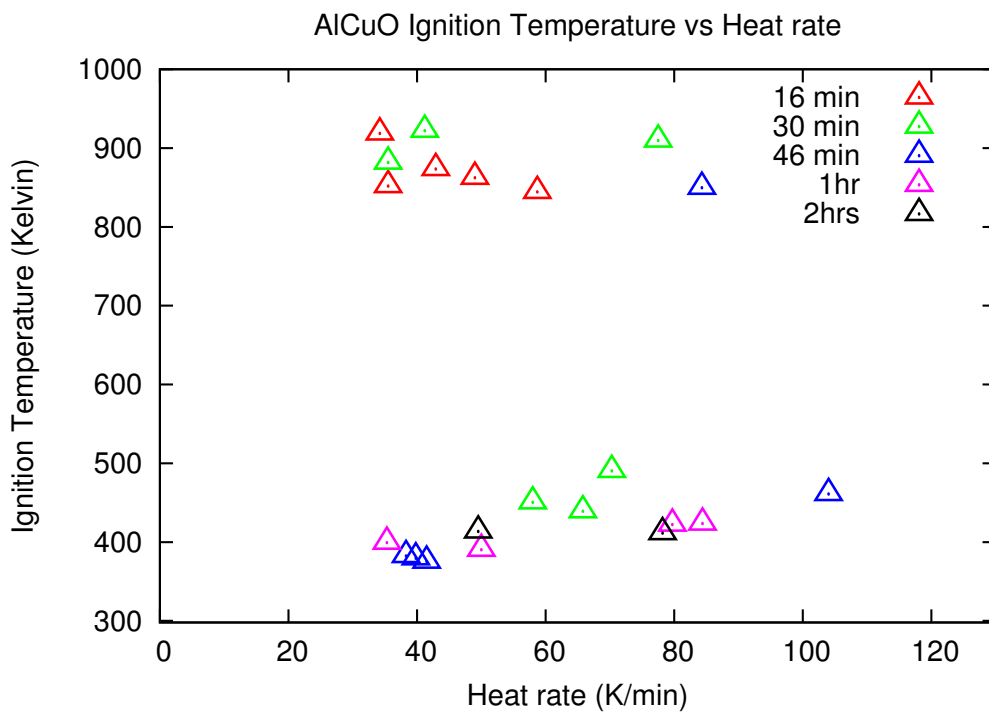


Figure 3.6: Ignition temperature vs heating rate for mixtures of milled Al-CuO

for a 60 minute milled system were in the range of 650-750 K when the sample was heated on a electrically heated wire. It must be noted that the range of heating rate when using the heated wire ignition method used by Umbrajkar et al. was 10^3 - 10^4 K/s, much higher than what was used in this study. According to Umbrajkar et al. [7] the ignition temperature increases as the heating rate is increased, which may explain the observed discrepancy. It is believed that the mechanically activated phases shown in figure 3.3 would lead to lower activation energies, and reduce the ignition temperatures. Umbrajkar et al. [7] reported activation energies of 106 kJ/mol for the decomposition of CuO into Cu₂O intermediate phase. It is believed that for this study, some pellets might have concentrations of these secondary phases high enough which would lead to ignition temperatures of 420-470 K. Pellets that did not have high concentrations of these intermediate phases reacted at 873 K. Figure 3.6 shows the ignition temperature plotted with respect to the heating rate. From these results, the transition seems to occur independently of the heating rate for the selected range that was permitted by the experimental setup. Mixtures of 30 minutes (green) and 46 minutes (blue), reacted in an inconsistent manner, and this behaviour is believed to be caused by intermediate phases and not the heating rate.

3.1.3 Flame Propagation

Flame propagation speeds were measured for milled mixtures of Al-CuO using the experimental setup described in section 2.4. Figure 3.7 shows a typical reconstruction of a flame propagation video for unmilled and milled mixtures of Al-CuO. By measuring the distance travelled by the flame front and dividing by the time between frames, the flame speed was calculated. Figure 3.8 shows the flame speed plotted with respect to the milling time. Flame speeds for an unmilled mixture of Al-CuO varied around 1 m/s. For a 16 minute milled system, the flame speeds was increased to approximately 80 m/s. Periods of milling longer than 16 minutes resulted in a decreasing trend in the flame propagation speed. This decrease is attributed to the presence of intermediate phases formed during milling.

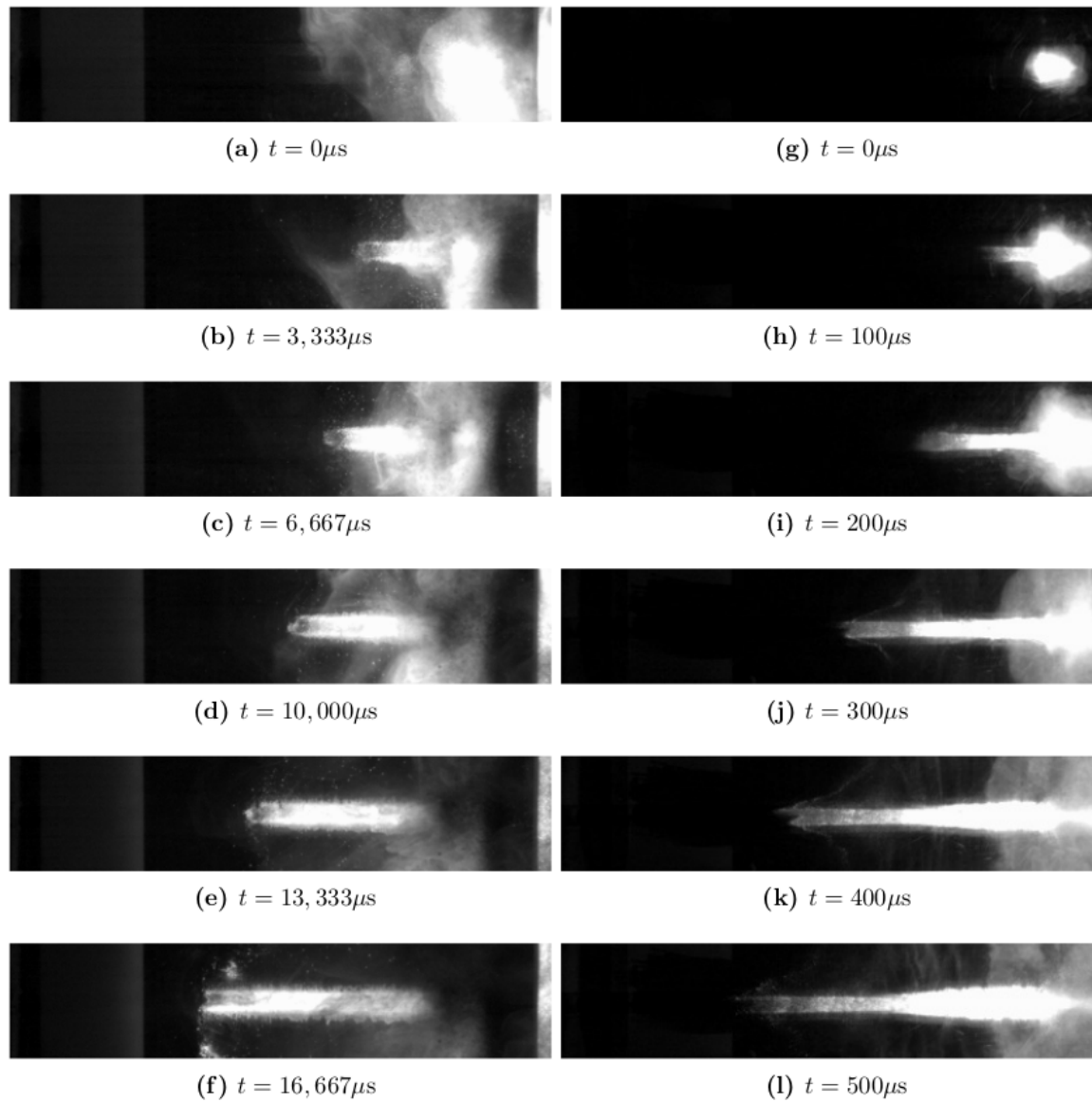


Figure 3.7: Reconstruction of flame propagation images for unmilled (a-f) and 16 minute milled powders (g-l) for Al-CuO mixtures demonstrating the flame front evolution as a function of time. From Maines et al. [30]

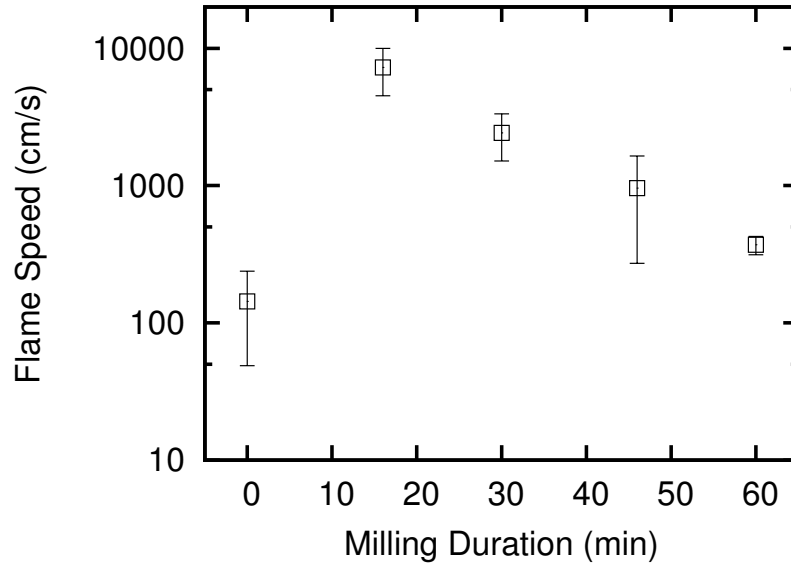


Figure 3.8: Average flame speeds related to milling time for Al-CuO

3.2 Ni-Al

Stoichiometric mixtures of Ni-Al were milled using settings described in table 2.1. The maximum milling time was set to 40 minutes. Bacciochini et al. [29] had shown that under the current mill settings, powders were mechanically activated at 42 minutes. Milling times for Ni-Al were set to 16, 30, and 40 minutes. The morphologies of unmilled Ni-Al powders are shown in figure 3.9. Figure 3.10 shows the cross sectional view of a 16 minute milled Ni-Al particle. At 16 minutes of milling, particles of Nickel are embedded in the aluminium matrix similar to what was seen for Al-CuO. Formation of elongated nickel lamelas was observed. The formation of these lamelas increased the surface contact ratio between constituents. The quantity of nano-laminates was increased for longer periods of milling. Figure 3.11 shows a cross section of a 30 minute milled Ni-Al particle. An increase in number of these laminates as well as a decrease in nickel particle size within the aluminium matrix is observed. Figure 3.12 shows the micro-structure of a 40 minute milled particle of Ni-Al. At 40 minutes of milling a much more refined micro-structure is observed. A 40 minute milled system of Ni-Al shows a constituent interface which is reduced down to a nano-scale. Figure 3.13 shows that although the particle interface between constituents

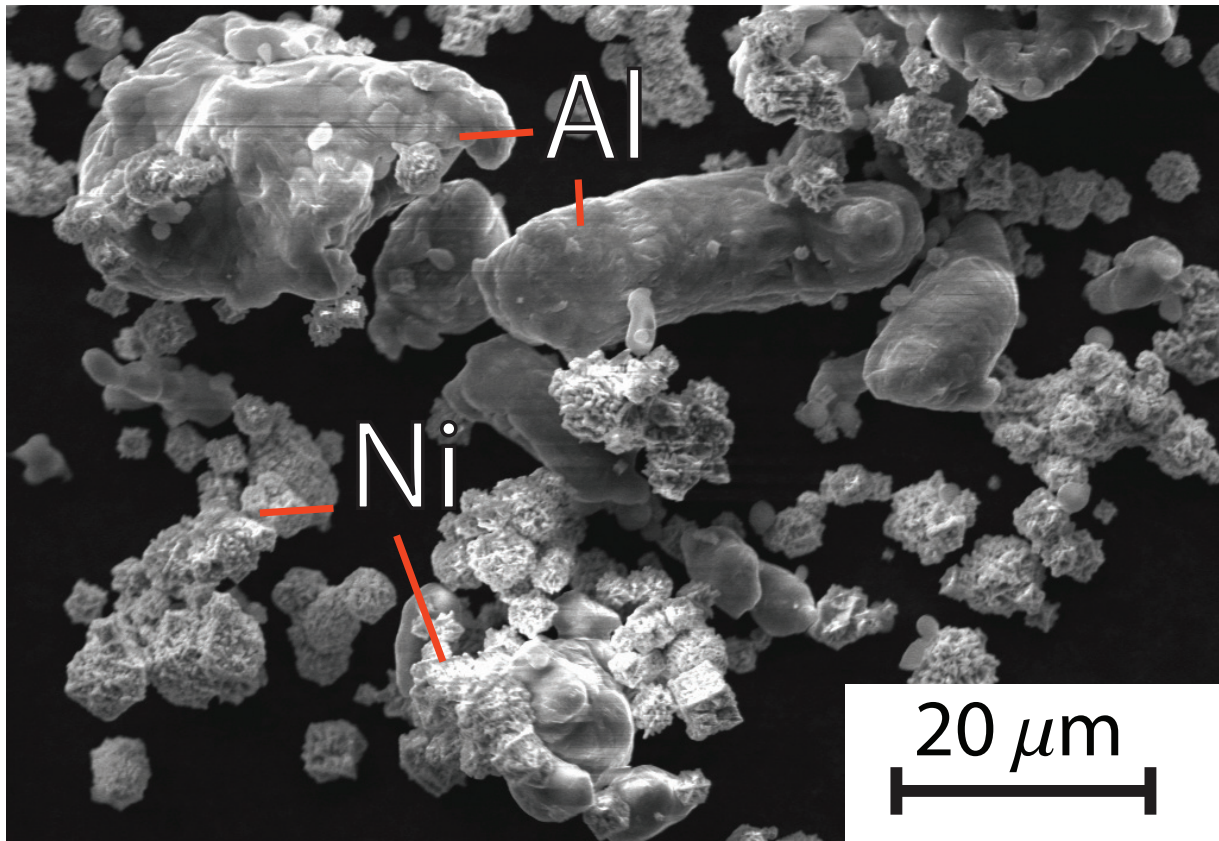


Figure 3.9: SEM image showing morphology and overall particle size of unmilled Ni-Al

was reduced to a nano-scale, the overall particle size of the milled powders remained on a micron-scale.

X-ray diffraction study results of unmilled and milled Ni-Al powders are shown in figure 3.14. When stoichiometric mixtures of Ni-Al were milled for 16, 30, and 40 minutes using the settings described in section 2, no secondary phases were formed. The suitable candidate for creating a hybrid can be Ni-Al milled for 16, 30, or 40 minutes. The mixture with lowest ignition temperatures will be used to create the hybrid mixture of Al-CuO-Ni.

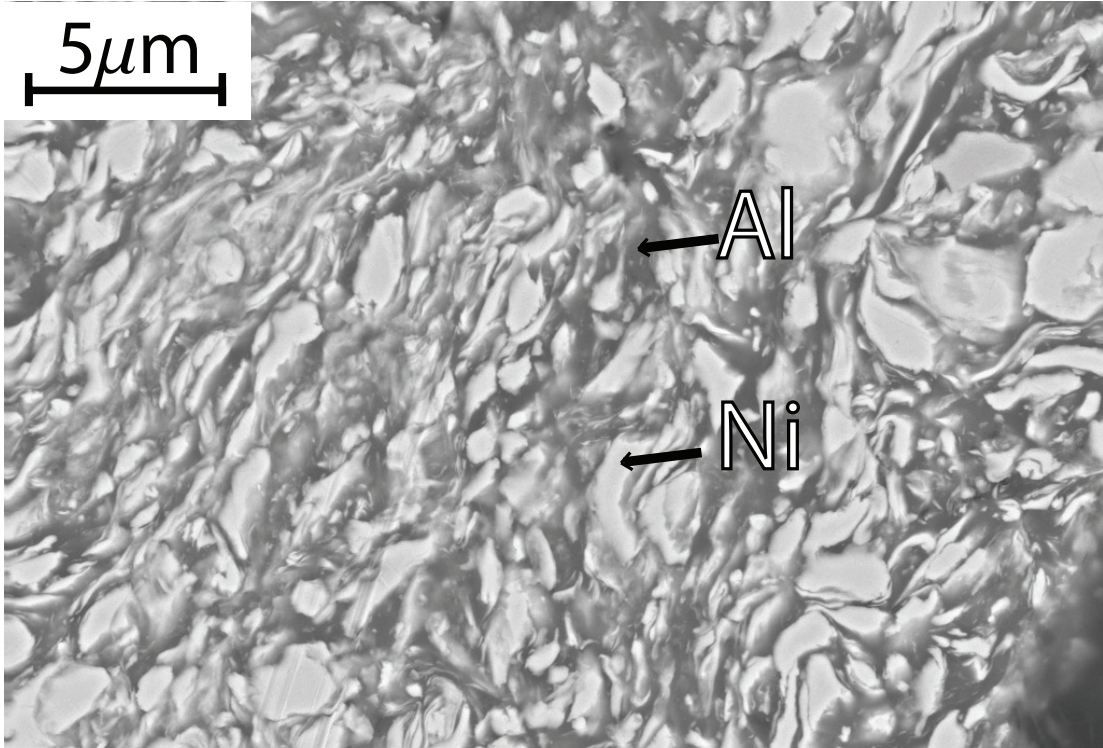


Figure 3.10: SEM cross-sectional view of 16 minute milled Ni-Al

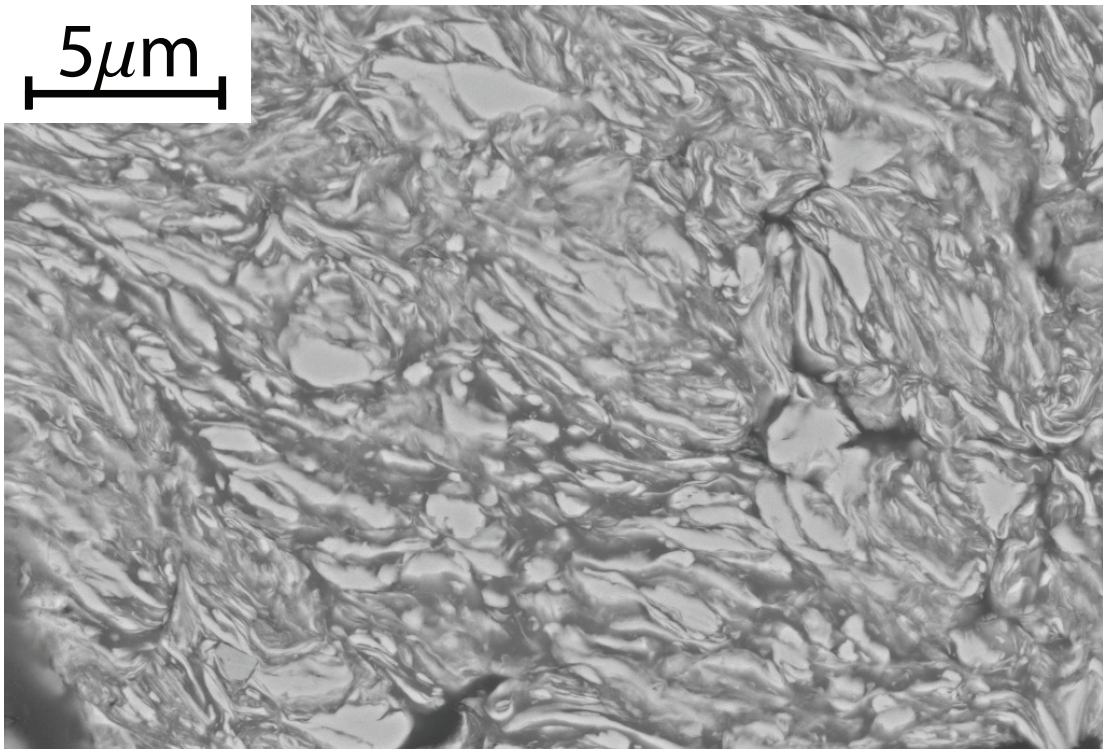


Figure 3.11: SEM cross-sectional view of 30 minute milled Ni-Al

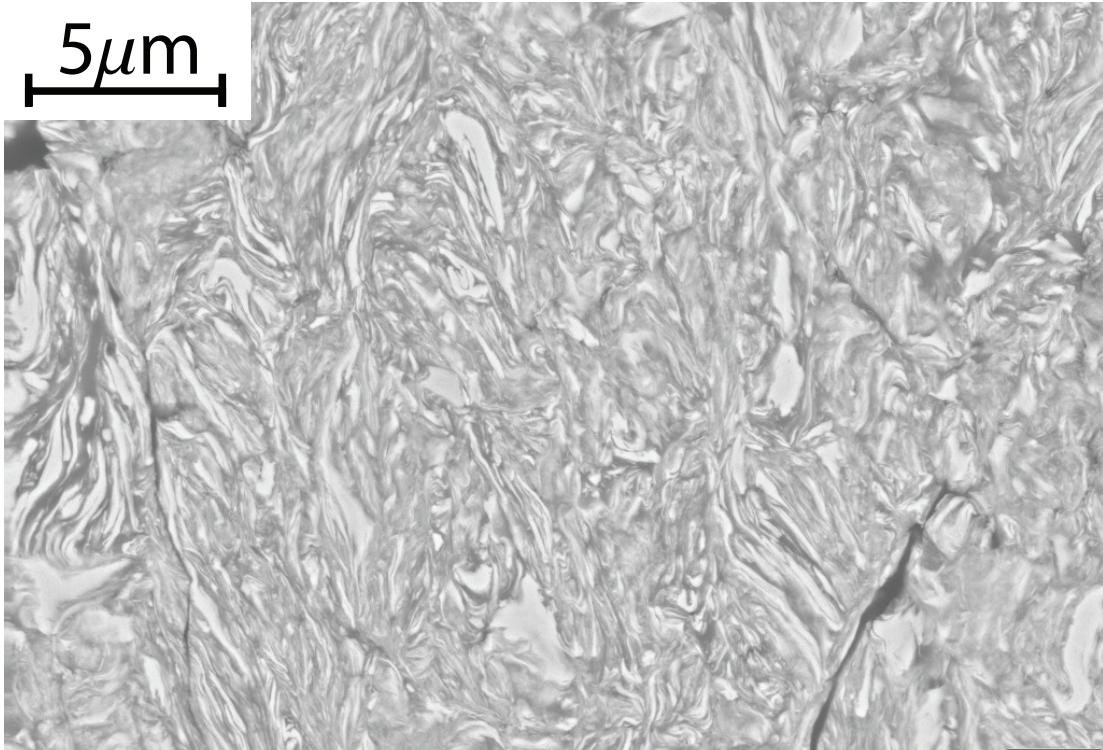


Figure 3.12: SEM cross-sectional view of 40 minute milled Ni-Al

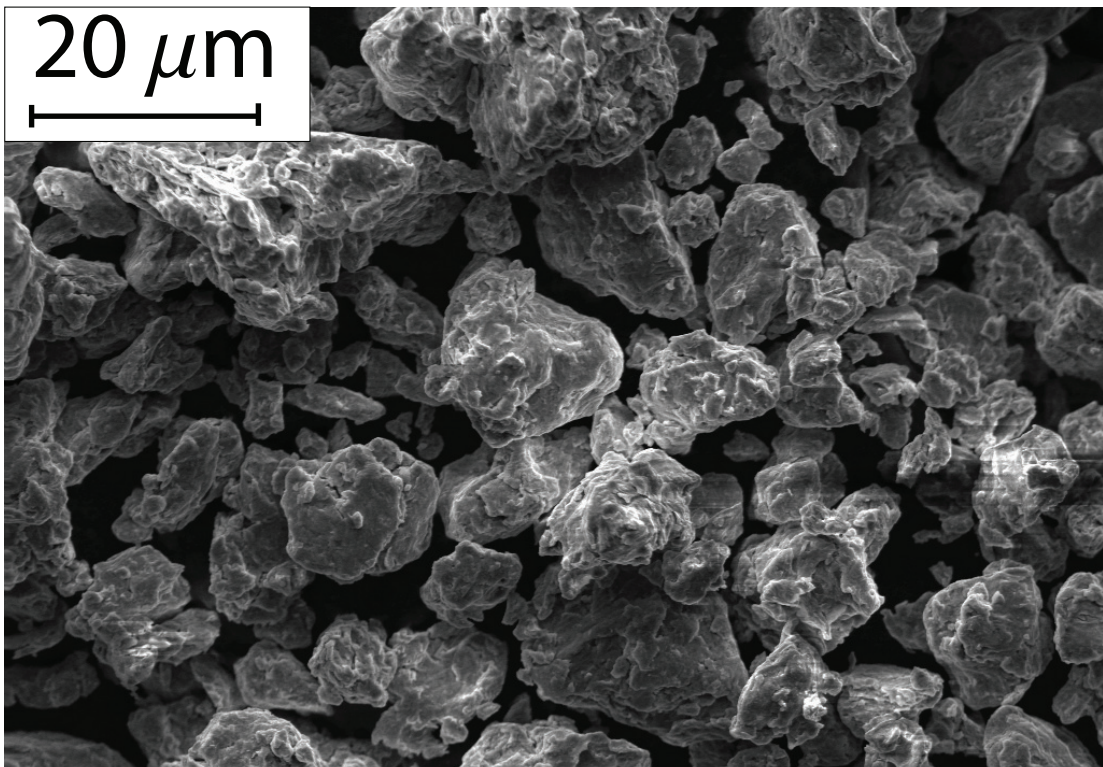


Figure 3.13: SEM image showing morphology and particle size of Ni-Al - 40 minutes milled

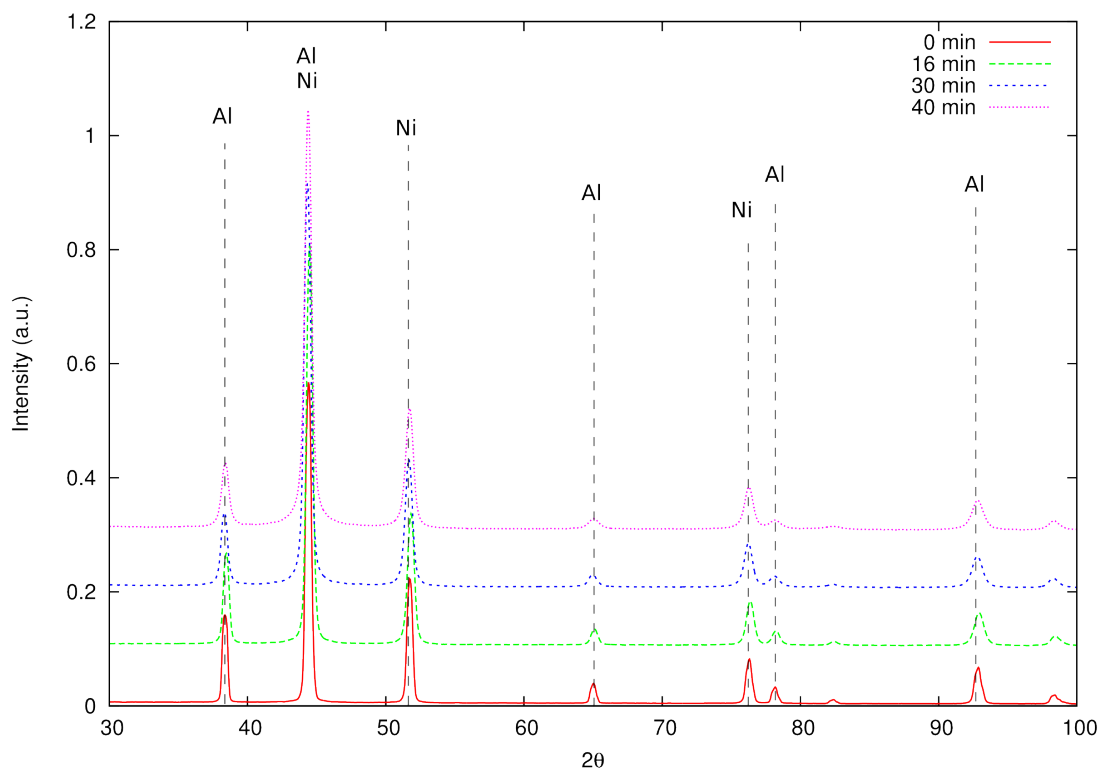


Figure 3.14: XRD study of unmilled and milled mixtures of Ni-Al powders

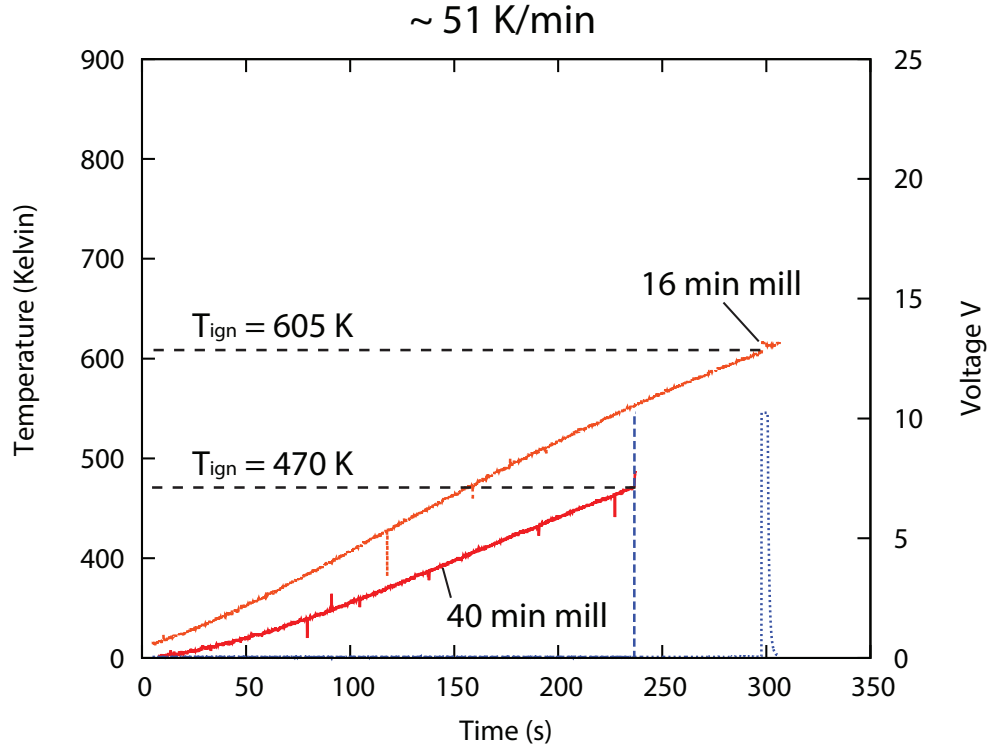


Figure 3.15: Temperature (red, orange) and voltage (blue) evolution with respect to time for 16 minute and 40 minute milled Ni-Al

3.2.1 Ignition Temperature

Mixtures of milled Ni-Al were tested in the experimental setup similarly to what was done for Al-CuO. A typical plot for the heating of Ni-Al obtained using this setup is shown in figure 3.15. The ignition event was characterized by an increase in temperature coinciding with a spike in voltage (blue). Figure 3.15 represents a case where the heating rate was approximately 51 K/min for both mill times. Heating rate was calculated by calculating the slope of the temperature evolution for the first 100 degrees before the ignition event. For the cases shown in figure 3.15, the ignition temperature were 605 K and 470 K for 16 minutes and 40 minutes respectively. Results for 30 minutes of milling yielded temperature and voltage evolution plots identical to what is shown in figure 3.15. Higher heating rates resulted in higher slopes, but the behaviour did not change.

The initial ignition temperature for unmilled Ni-Al was shown by Manukyan et al. [20] to be approximately 913 K. Figure 3.16 shows the ignition temperature results for milled

mixtures of Ni-Al. Our study shows that a 16 minute milled system of Ni-Al has average ignition temperature of 625 K. Longer periods of milling time further reduces the ignition temperatures. The decrease in ignition temperatures for milling times between 16 minutes and 40 minutes seems to follow a linear trend. The lowest average ignition temperature obtained was 480 K for a 40 minute milled Ni-Al mixture.

Figure 3.17 shows the ignition temperatures plotted with respect to the heating rate. Ignition temperatures for a mill time of 16 minutes show no clear dependency on the heating rate for the range of heating rates used in this study. Mixtures of 30 minute milled Ni-Al show a transition similar to Al-CuO occurring between 38 and 65 K/min where the ignition temperature is either 600 K or approximately 490 K. For heating rates higher than 65 K/min, the ignition temperature of a 30 minute milled mixture remains at approximately 490 K. The cause for this transition remains unknown since no secondary phases were present, as shown by XRD (figure 3.14). A 40 minute milled mixture of Ni-Al has ignition temperatures relatively consistent at 480 K, and is shown to be independent of the heating rate. This result is slightly lower than what Manukyan et al. [20] had reported. They found that for a mill time of 17 minutes dry milling, and 10 minutes of wet grinding, the ignition temperatures were approximately 500 K.

The ideal candidate chosen to lower the ignition temperature of Al-CuO was a 40 minute milled system of Ni-Al. A mixture of 40 minute milled Ni-Al has ignition temperatures averaging 480 K, and no secondary phases were reported.

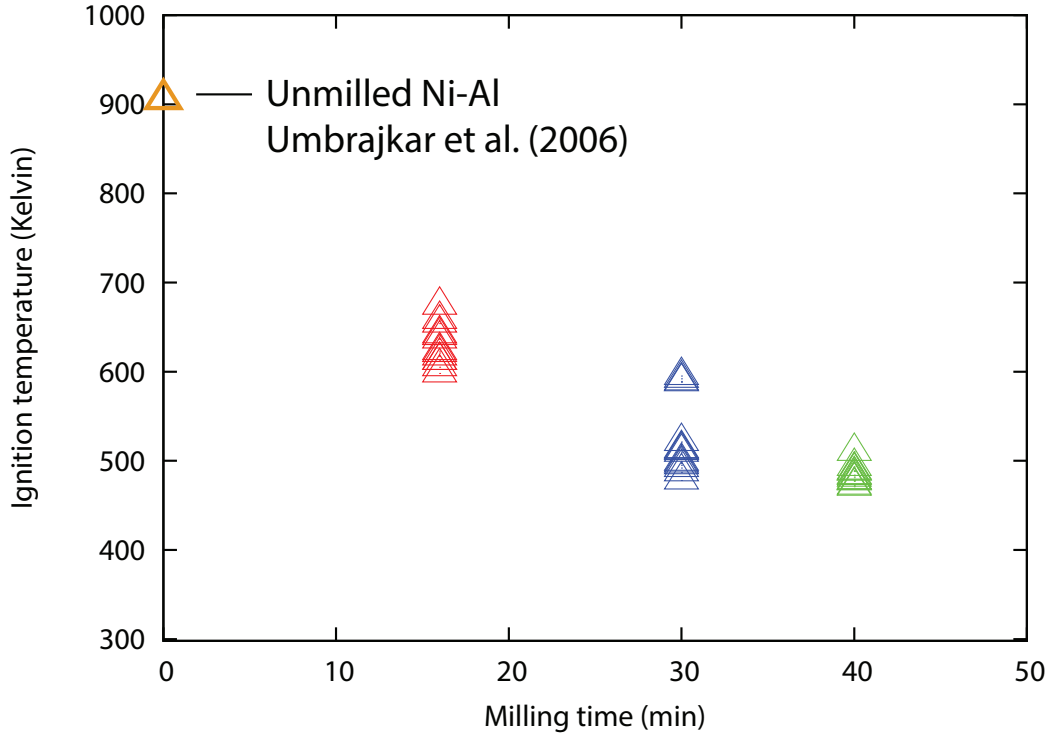


Figure 3.16: Ignition temperatures vs mill time for mixtures of milled Ni-Al

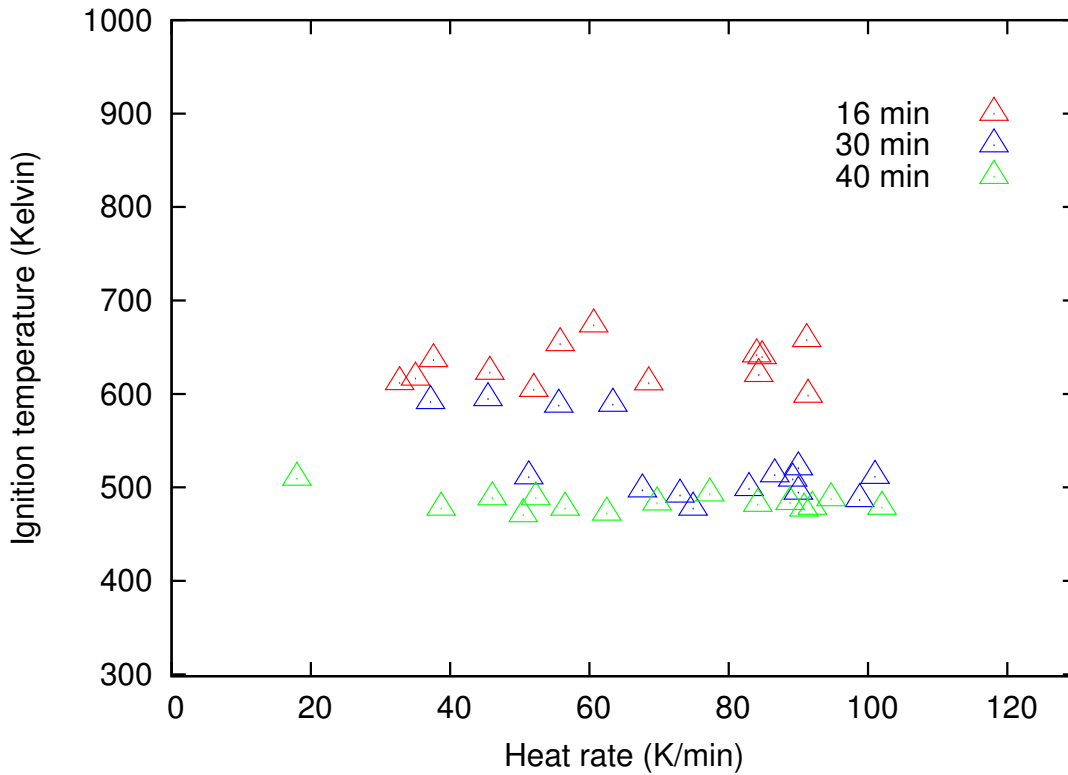


Figure 3.17: Ignition temperatures vs heating rate for mixtures of milled Ni-Al

3.3 Hybrid Mixture - Hand mixed

3.3.1 Morphology

The objective of creating a hybrid mixture is to reduce the ignition temperature of Al-CuO using a compound with lower ignition temperatures. A mixture of 16 minute milled Al-CuO was used to create the hybrid mixture as it proved to have more refined micro-structure, showed no secondary phases, and had higher flame speeds than unmilled Al-CuO. The candidate chosen to reduce the ignition temperature of Al-CuO was a 40 minute milled mixture of stoichiometric Ni-Al powders. The 40 minute mixture of Ni-Al yielded average ignition temperatures of 480 K as shown in section 3.2, significantly lower than unmilled Ni-Al (913 K) [7]. Powders of 16 minute milled Al-CuO and 40 minute milled Ni-Al were hand mixed at varying concentrations with respect to mass. Once the hand mixed mixture of Al-CuO-Ni was created, the microstructure was analysed using SEM. Figure 3.18 represents a case of 50% by mass of 40 minute milled Ni-Al with 16 minute milled Al-CuO. All concentrations of these hand mixed mixtures had micro-structures similar to what is shown in figure 3.18. Since no mechanical alloying was performed, the respective microstructures of both constituents did not vary from figure 3.12 and figure 3.2. Since the phase concentrations of mixtures of 16 minute Al-CuO and 40 minute Ni-Al have been analysed using XRD in sections 3.1 and 3.2, the phases present in the hand mixed hybrid mixtures were assumed to be identical.

3.3.2 Ignition

Ignition temperatures for hand mixed hybrid mixtures of Al-CuO-Ni were determined using the experimental apparatus shown in section 2. The temperature evolution inside the furnace followed the same trend as shown in figures 3.4 and 3.15.

Figure 3.19 shows the ignition temperature results plotted with respect to the added 40 minute milled Ni-Al mass fraction. A case of 0% Ni-Al mass fraction represents pure 16 minute Al-CuO, and 100% mass fraction represents pure 40 minute Ni-Al. Ignition

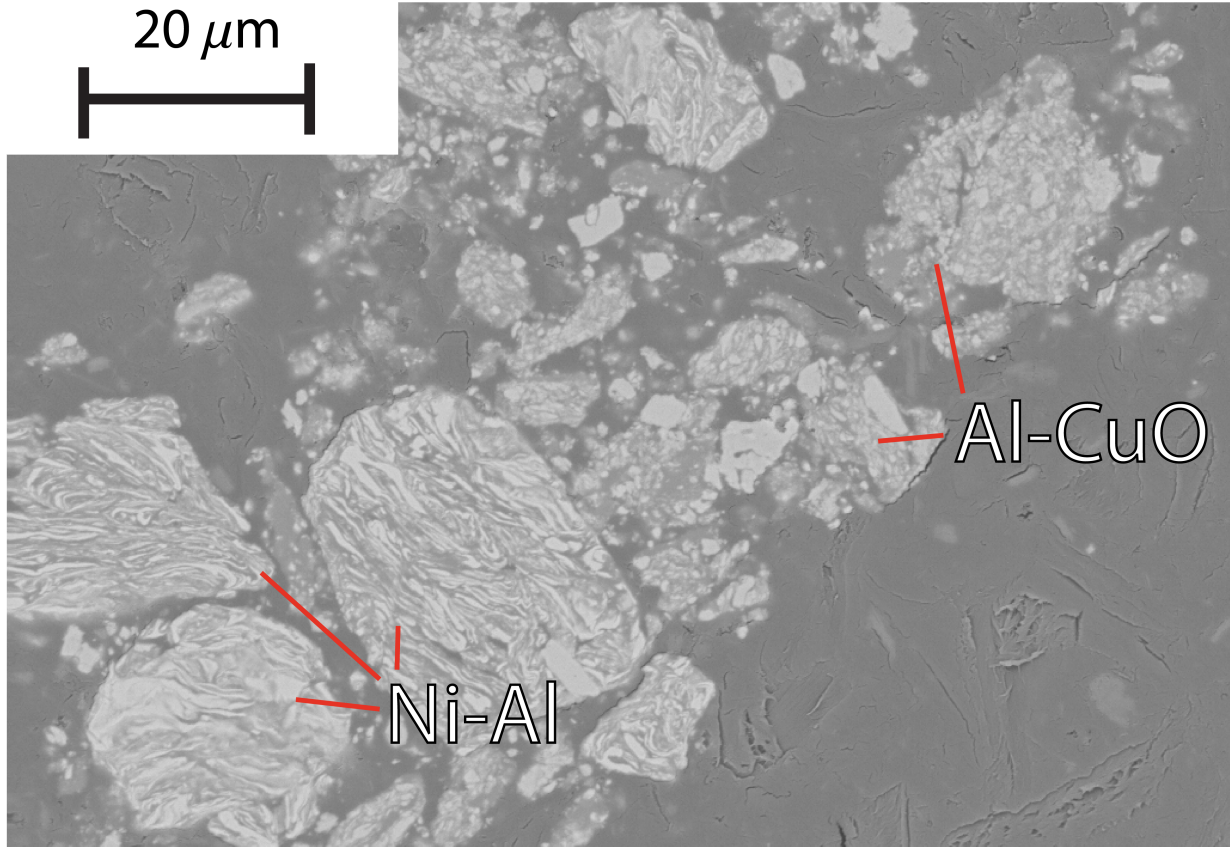


Figure 3.18: Typical morphology of hand mixed 50% 40 min Ni-Al and 50% 16 min Al-CuO hybrid mixture

temperatures for a pure 16 minute milled Al-CuO system averaged at 873 K. The hypothesis was that by creating a hybrid mixture one could directly control the ignition temperature of Al-CuO by adding varying concentrations of Ni-Al. Results from figure 3.19 show that adding 25% and 50% does not change the ignition temperatures. The hypothesis is that the heat generated by the material with lower ignition temperature (Ni-Al) was not enough to overcome the heat losses. At 65%, the ignition temperature was decreased to 500-620 K. The wide range of ignition temperature can be attributed to the hand mixing procedure, which offers poor mixing compared to ARM. A 75% concentrations had results nearly identical to adding 65%, but showed slightly lower ignition temperatures. From these results, we find that a hand mixed system of 16 minute Al-CuO and 40 minute Ni-Al requires a concentration of 65% Ni-Al by mass for ignition temperatures to be lower.

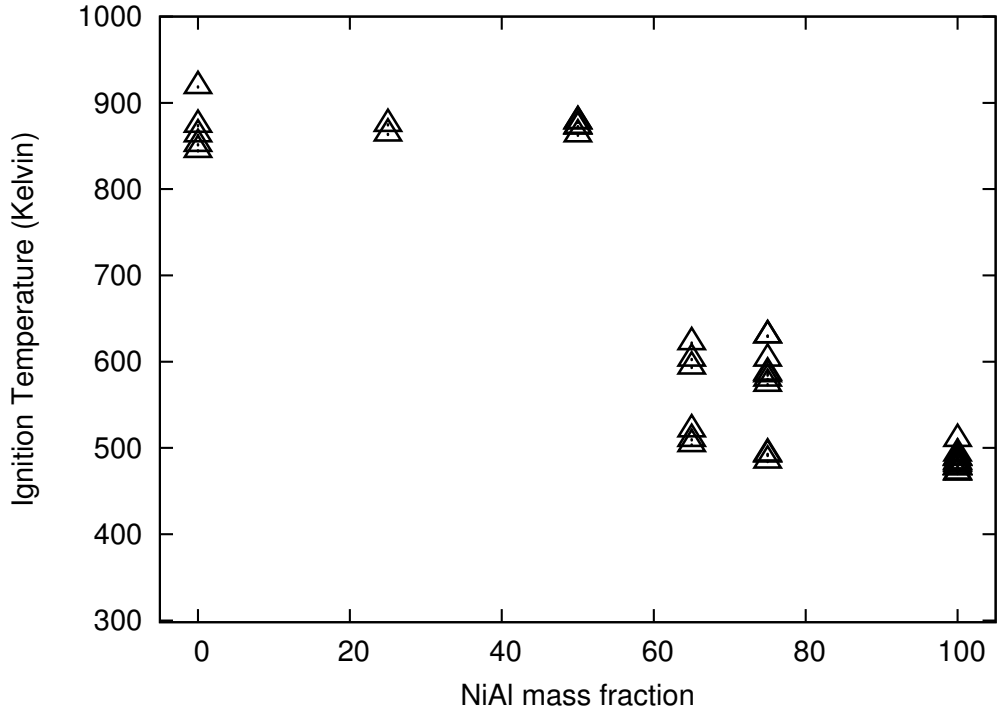


Figure 3.19: Unmilled hybrid mixture ignition temperature plotted with respect to the added Ni-Al mass fraction

Figure 3.20 shows the ignition temperatures plotted as a function of the heating rate. The ignition temperatures show no clear dependency on the heating rate for mixtures of 25 and 50% Ni-Al. The same transitional behaviour that was observed for Al-CuO and Ni-Al mixtures is captured for concentrations of 65 and 75%. The ignition temperatures seem to be either 570-600 K, or 480-500 K. This transitional phase seems independent of the heating rate, and the cause is unclear at this point.

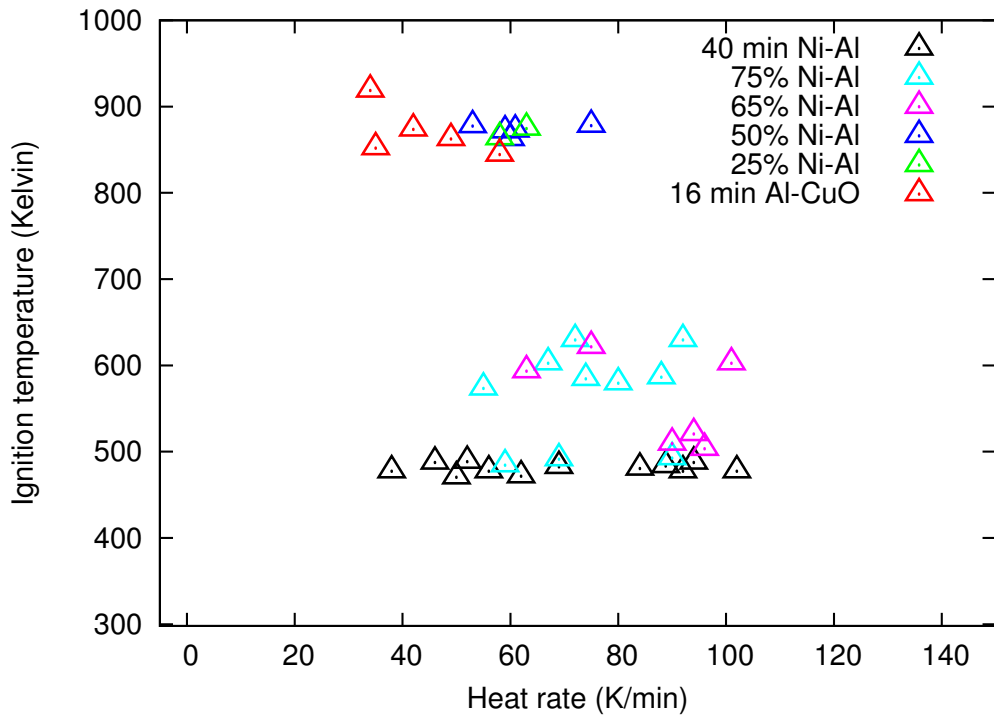


Figure 3.20: Unmilled hybrid mixture ignition temperature plotted with respect to the heating rate

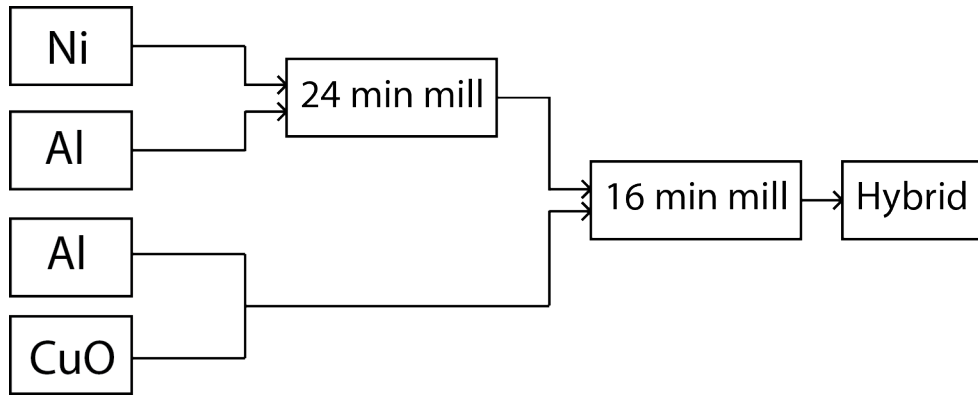


Figure 3.21: Milled hybrid mixture procedure

3.4 Hybrid Mixture - Milled

3.4.1 Hybrid Mixture Procedure

The procedure for creating a hybrid Al-CuO-Ni mixture was strongly dependent on the results of individual Al-CuO and Ni-Al mills previously shown in this chapter. The objective of the hybrid mixture was to create a compound that embodies the low ignition of the intermetallic Ni-Al with the high reactivity of Al-CuO without the negative effects of having intermediate phases. The candidate for this mixture was 16 minute milled Al-CuO due to its lower ignition temperature of 873 K and high reactivity. A 40 minute milled Ni-Al which had ignition temperatures of 480 K was chosen as the additive with lower ignition temperatures. One option was to create a mixture of 16 min Al-CuO and 40 min Ni-Al simply by hand mixing them together. The second option was to create a mechanically milled hybrid mixture with these total milling times. A milled hybrid mixture was created by milling raw Ni-Al for 24 minutes. The newly made 24 minute milled Ni-Al was then mixed with unmilled stoichiometric Al-CuO and milled for an additional 16 minutes. Mixtures were made at varying concentrations of constituents (25, 50 and 75% of added Ni-Al by mass). The mixture had a total of 40 minutes of milling for the Ni-Al compound, and a total of 16 minutes for the Al-CuO. Figure 3.21 shows a schematic of the steps taken to create a milled hybrid mixture.

3.4.2 Morphology

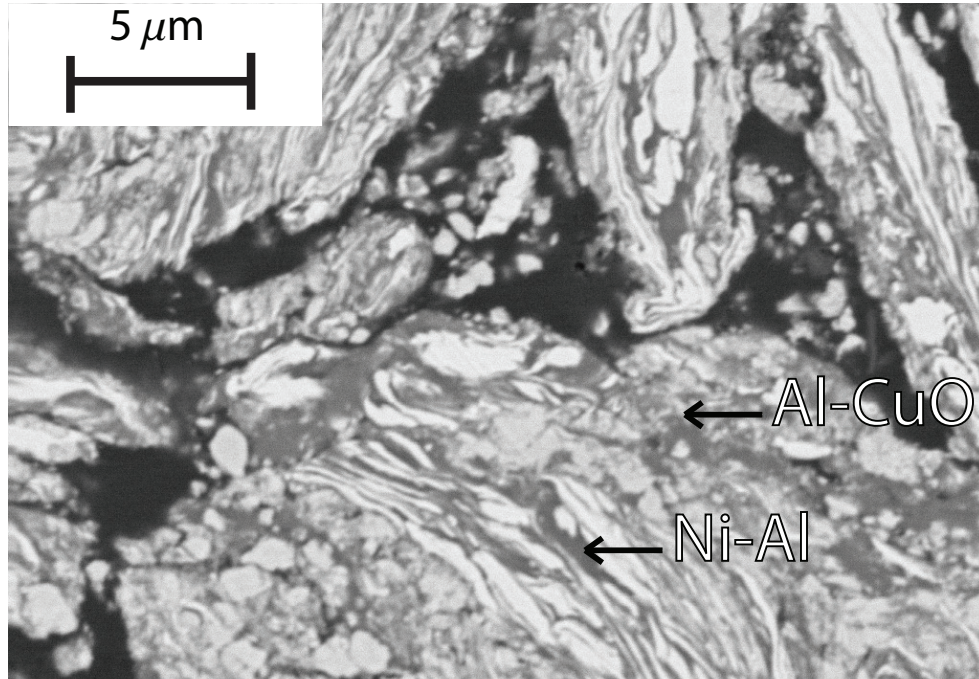


Figure 3.22: Typical SEM cross-sectional view of a milled hybrid mixture

Following the procedure explained in section 3.4.1, the micro-structure of the milled hybrid system was analysed using scanning electron microscopy (SEM). Figure 3.22 shows the typical cross sectional micro-structure of a milled hybrid system. The elongated lamellas of nickel that were present in pure 40 minute milled Ni-Al are clearly visible in this milled hybrid mixture, and can easily be distinguished apart from the copper-oxide particles. An EDS study was performed which allowed one to confirm the distinction between Al, CuO, and Ni. Both nickel and copper-oxide were embedded in the aluminium matrix, similar to what was seen previously in this chapter. A milled system of Al-CuO-Ni shows constituents intermixed relatively evenly. The coarse particle size of a milled hybrid system remained on the order of 5-30 microns. XRD results are shown in figure 3.23. X-ray diffraction showed that no secondary phases were formed during the milling procedure.

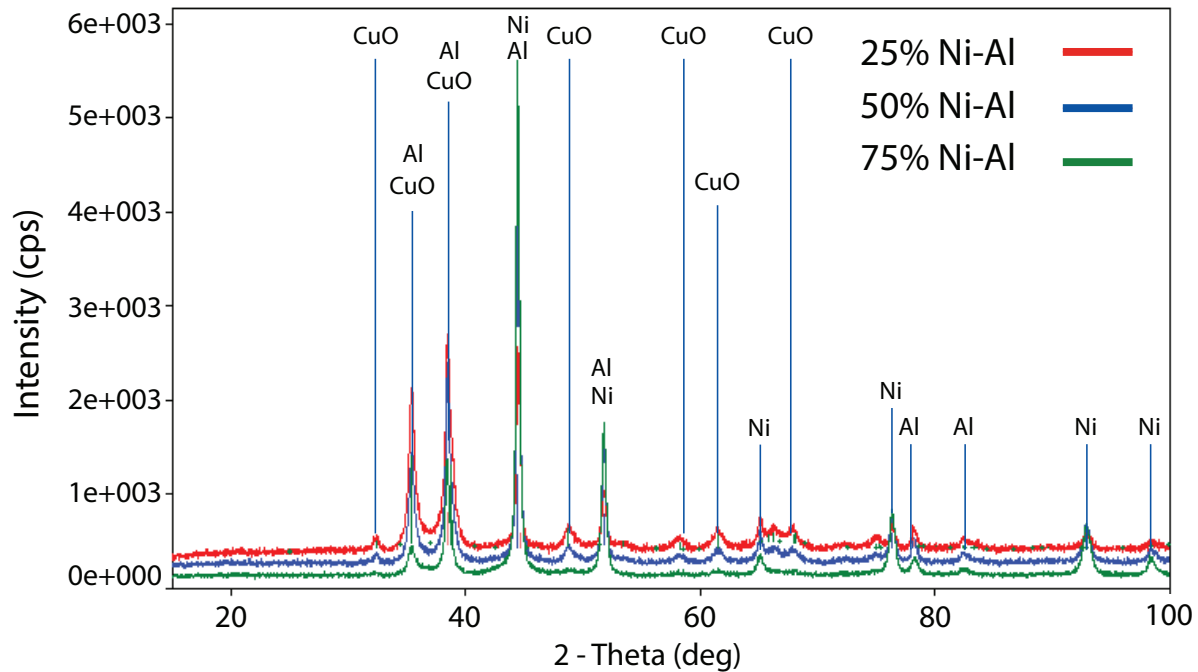


Figure 3.23: X-ray diffraction study results of a milled Al-CuO-Ni system at concentrations of 25%, 50%, and 75% added Ni-Al mass fraction

3.4.3 Ignition

The temperature evolution plots for the milled hybrid mixture are shown in figure 3.24. The general evolution of temperature with respect to time, remains identical to the mixtures of Al-CuO and Ni-Al. Figure 3.25 show the ignition temperature results for a milled hybrid system at varying concentrations of added Ni-Al. Results in figure 3.25 show that while the ignition temperature of a milled system is dependent on the added concentration of Ni-Al, a specific amount of Ni-Al is required to decrease the ignition temperature of the system. When 25% of Ni-Al is added, both the milled and unmilled system behave identically to that of a pure 16 minute milled Al-CuO system with ignition temperatures of 873 K. Only after 50% of added Ni-Al by mass does the ignition temperature of the milled hybrid mixture decrease. The ignition temperature is decreased to 620-750 K. After 75% of Ni-Al is added, ignition temperatures vary between 480-600 K, slightly lower than the unmilled hybrid system. There appears to be a more gradual trend with respect to the added concentration of Ni-Al in the case of a milled hybrid system. For the unmilled

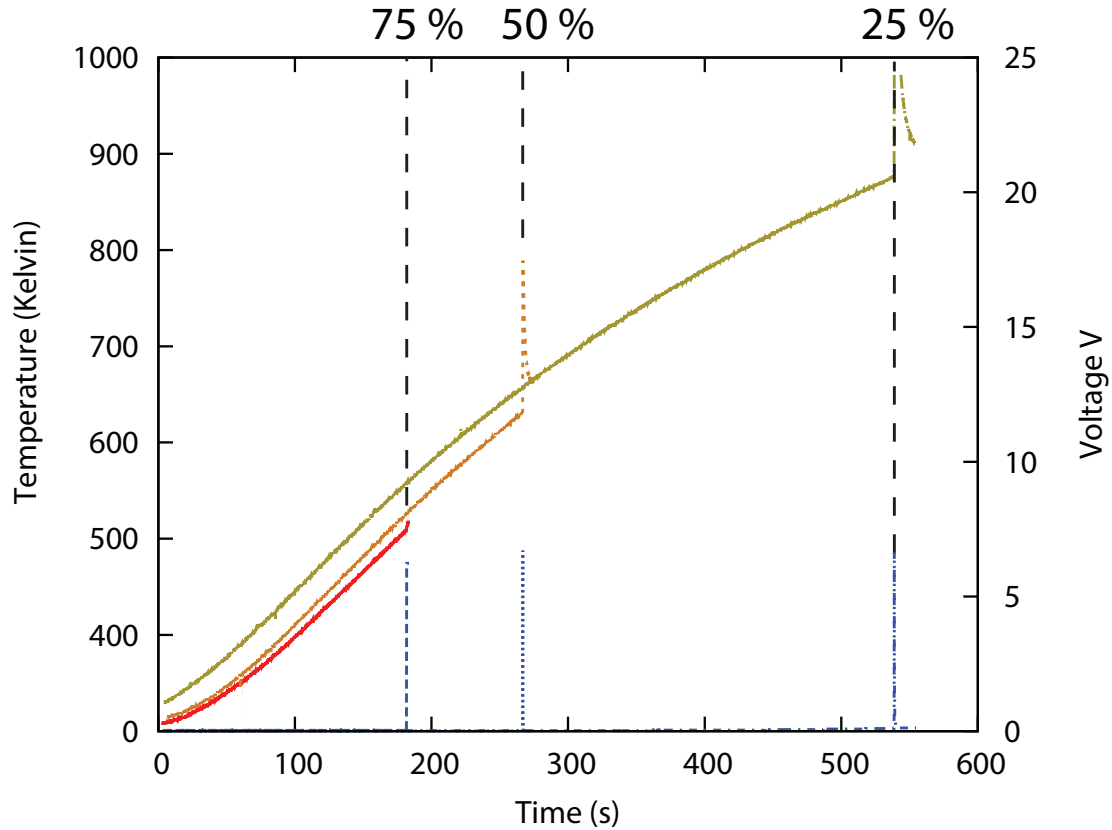


Figure 3.24: Temperature and voltage (blue) evolution for milled hybrid mixtures of Al-CuO-Ni at concentrations of 25, 50 and 75 percent of Ni-Al by mass

hybrid system, there appears to be a more abrupt decrease in the ignition temperature that occurred at 65% of added Ni-Al (figure 3.19).

Figure 3.26 shows the ignition temperatures plotted as a function of the heating rate for a milled hybrid system. At 50% concentration of Ni-Al at a heating rate of 80 K/min, ignition results fluctuated between 750 K and 620 K. The ignition temperature of a 75% Ni-Al mixture varied between 473-570 K at heating rates of 70 K/min. It appears that lower heating rates lead to the transitional behaviour in the ignition temperatures. Higher heating rates lead to more consistent results, favouring the lower range of ignition temperatures. The cause for this transition is unknown since no secondary phases were present, as shown in figure 3.23.

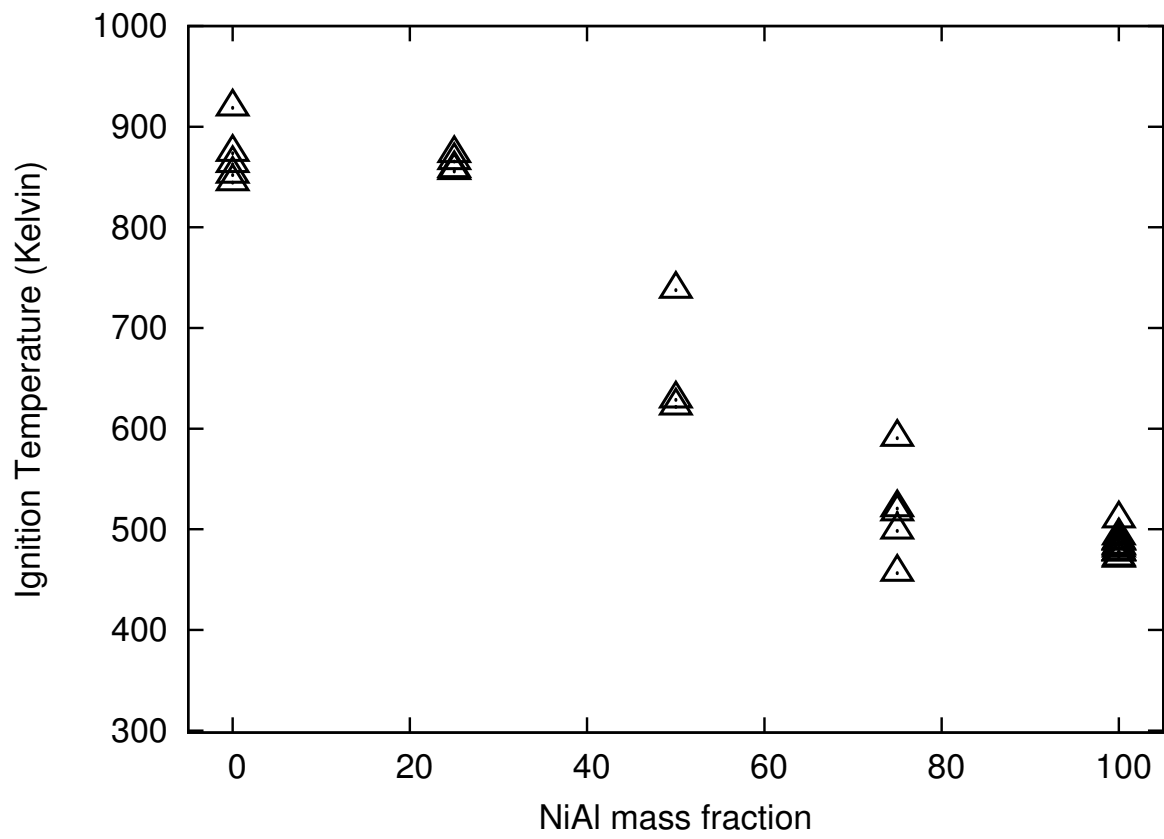


Figure 3.25: Milled hybrid mixture ignition temperature results for varying mass fractions of Ni-Al

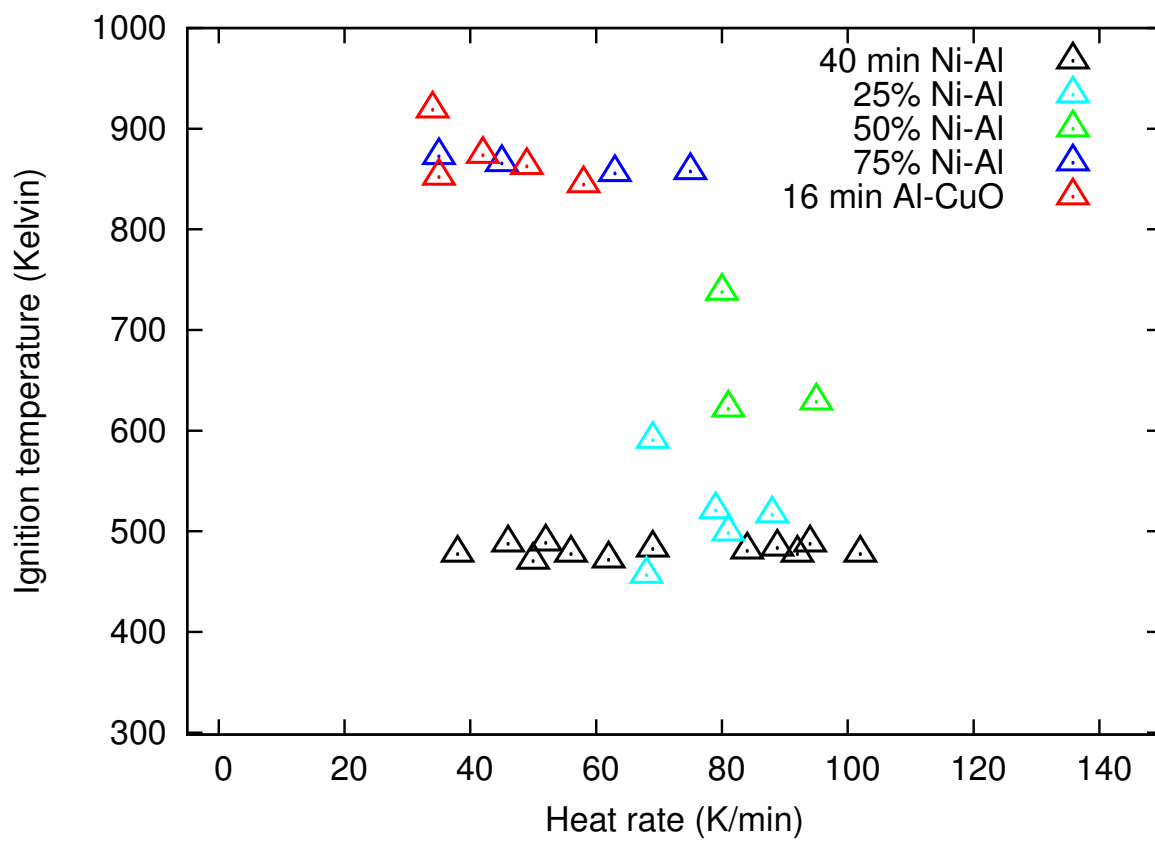


Figure 3.26: Milled hybrid mixture ignition temperature plotted with respect to the heating rate

Chapter 4

Ignition Model

To simplify the ignition model, we assume that the temperature is uniform through a pellet of Ni-Al or Al-CuO. In order to justify the lumped capacitance analysis (LCA), the Biot number is calculated. The Biot number is given by

$$Bi = \frac{hL_c}{k_b} \quad (4.1)$$

Here L_c is the characteristic length of the pellet (volume divided by surface area), and k_b is the thermal conductivity. The convection coefficient h was calculated using a method following Holman's Heat Transfer [31].

$$\frac{hd}{k_f} = cRe_f^n Pr_f^{\frac{1}{3}} \quad (4.2)$$

$$Re = \frac{\rho u_\infty d}{\mu} \quad (4.3)$$

$$Pr_f = \frac{c_p \mu}{k_f} \quad (4.4)$$

Where h is the convection coefficient, d is the diameter of the pellet, and k_f is the conductivity of argon. The speed of the flow u_∞ is 0.00065m/s , given by the flow meter shown in the experimental set-up. Values for c and n were taken from Holman [31] on page 297 and set to 0.989, and 0.330 respectively. The characteristic length (volume divided by surface area) of a pellet used in the experiments was $7.5 \cdot 10^{-4}\text{m}$. Thermal conductivity (k_b) for reactive metal powder was taken from Akbarnejad [32] and set to 2 W/mK . The

calculated convective heat transfer coefficient h was approximately $5 \frac{W}{m^2K}$. The resulting Biot number was on the order of 10^{-3} , much smaller than 1, which means that the heat transfer inside a heated pellet happens much more rapidly than the heat transfer at the surface. Lumped capacitance was therefore implemented for the ignition model.

4.1 Single Phase System

Arrhenius type reaction models are widely used in literature to model the reaction kinetics of reactive materials [10, 21, 33, 34]. The ordinary differential equations for a single phase system is

$$mC_v \frac{dT}{dt} = mQ_R \lambda \exp\left(-\frac{E_a}{RT}\right) - hA(T - T_\infty) - \sigma \varepsilon A (T^4 - T_\infty^4) \quad (4.5)$$

$$\frac{d\lambda}{dt} = -Z \lambda \exp\left(-\frac{E_a}{RT}\right) \quad (4.6)$$

$$\frac{dT_\infty}{dt} = K \quad (4.7)$$

Here C_v is the heat capacity, m is the mass of the pellet, Q_R is defined as the energy heat release, E_a is the activation energy, h is the convection coefficient, and A is the surface area of the pellet. The term σ is the Stefan-Boltzmann constant, and ε is the emissivity of the pellet. The concentration of reactants, λ , goes from 1 at ($t = 0$) to 0 when reaction is complete. The term K is the heating rate of the system.

4.1.1 Parameters

Shteinberg et al. [35] studied the effects of high energy ball milling on the activation energy of Ni-Al. Mill settings, heat rate, and powder morphology was very similar to what has been done for this thesis. Following DSC experiments, the Kissinger method was used to calculate the activation energy of the milled powders. Results showed that for a stoichiometric milled Ni-Al system, the activation energy is 104 kJ/mol. Similarly, Umbrajkar et al. [7] found that the activation energy for a 16 minute milled system of Al-CuO is 277 kJ/mol. The value for Q_R for each compound was taken from Fischer et

Table 4.1: Parameters used in the ignition model for individual mixtures of Al-CuO and Ni-Al

Parameters	Ni-Al	Al-CuO
E_a (kJ/mol)	104	277
h ($\frac{W}{m^2K}$)	5	5
Q_R ($\frac{J}{g}$)	1300	4077
C_v ($\frac{J}{gK}$)	0.588	0.653
ε	0.1	0.5

al.[1]. The emissivity was averaged for Al (0.1), Ni (0.1), and CuO (0.83) from [36]. The initial conditions are $\lambda = 1$, $\frac{dT_\infty}{dt} = 60$ K/min, and $T = T_\infty = 300K$. The heating rate K was set to 50 K/min. Parameters used for each mixtures are shown in table 4.1

The Arrhenius pre-exponential factor remains the only unknown. The pre-exponent is a tunable factor which is usually tuned to make the model match experimental results [10, 21]. The system of ODEs were integrated numerically using *Mathematica*. The code used for this work is shown in Appendix A.

Figure 4.1 represents a typical temperature evolution with respect to time for Al-CuO, given different values of the Arrhenius pre-exponent Z . As the pre-exponential factor increases, the ignition occurs sooner, and at lower ignition temperatures. The value of Z was incremented until the ignition temperature matched the pure 16 minute milled Al-CuO experimental data. As shown in figure 4.1, the resulting Z found for Al-CuO was $Z = 10^{14}$. Figure 4.2 shows the temperature (blue) and concentration (red) evolution with respect to time for the case where $Z = 10^{14}$.

Figure 4.3 shows the evolution of temperature with respect to time, for the ignition model applied to Ni-Al. The same trend that was observed for Al-CuO is captured for Ni-Al. As the pre-exponential factor is increased from $Z = 5 \times 10^5$ to $Z = 5 \times 10^8$, the ignition temperature decreases. Figure 4.4 shows the evolution of temperature and concentration for which the ignition temperature matched the experimental data of 40 minute milled Ni-Al. The final value of the pre-exponent for Ni-Al is $Z = 5 \times 10^8$.

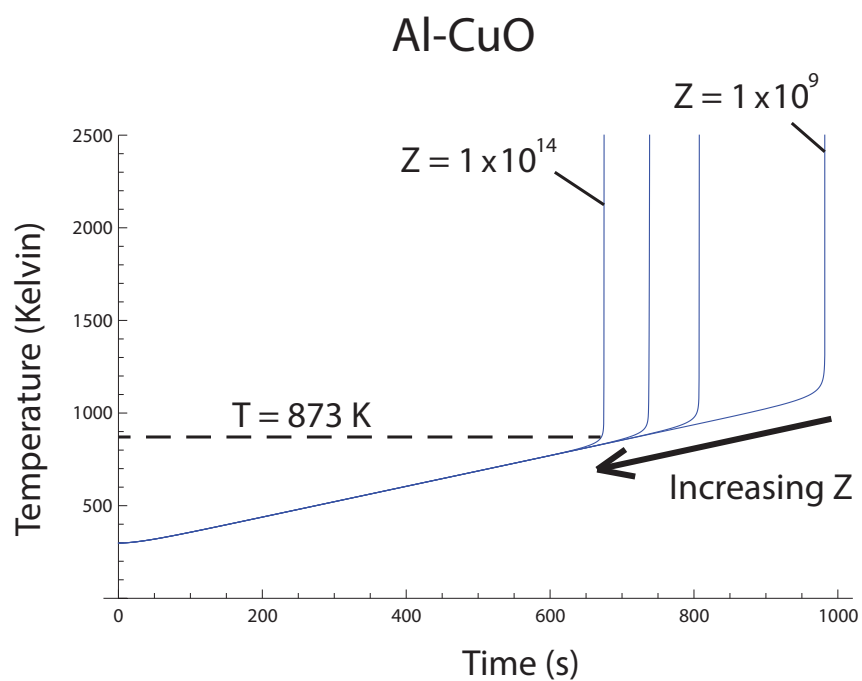


Figure 4.1: Ignition model for Al-CuO for varying values of pre-exponential factor Z

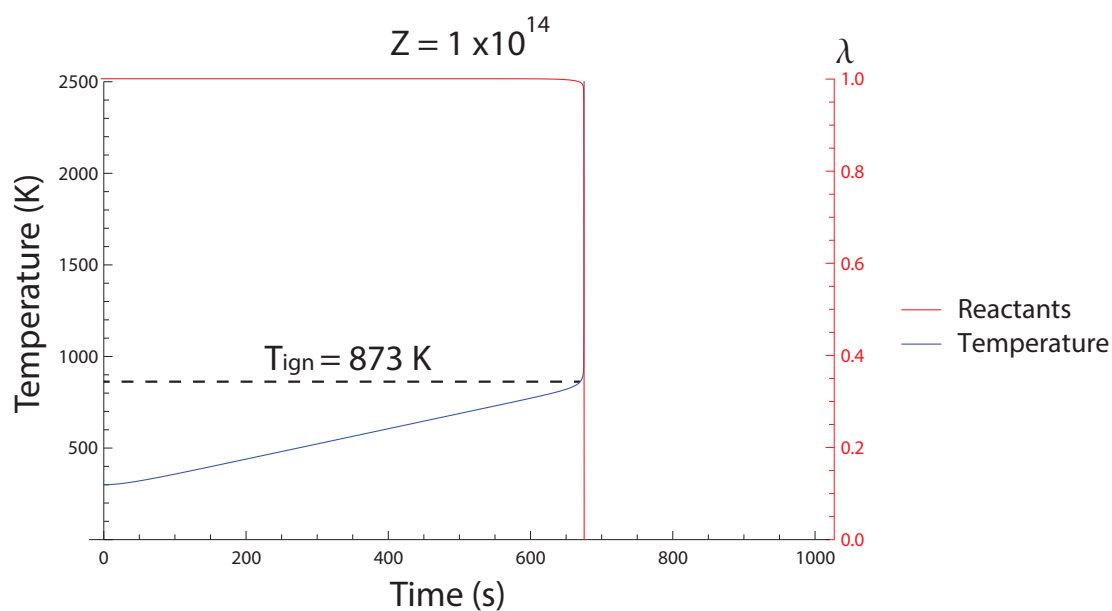


Figure 4.2: Temperature (blue) and concentration (red) evolution with time of Al-CuO from the ignition model

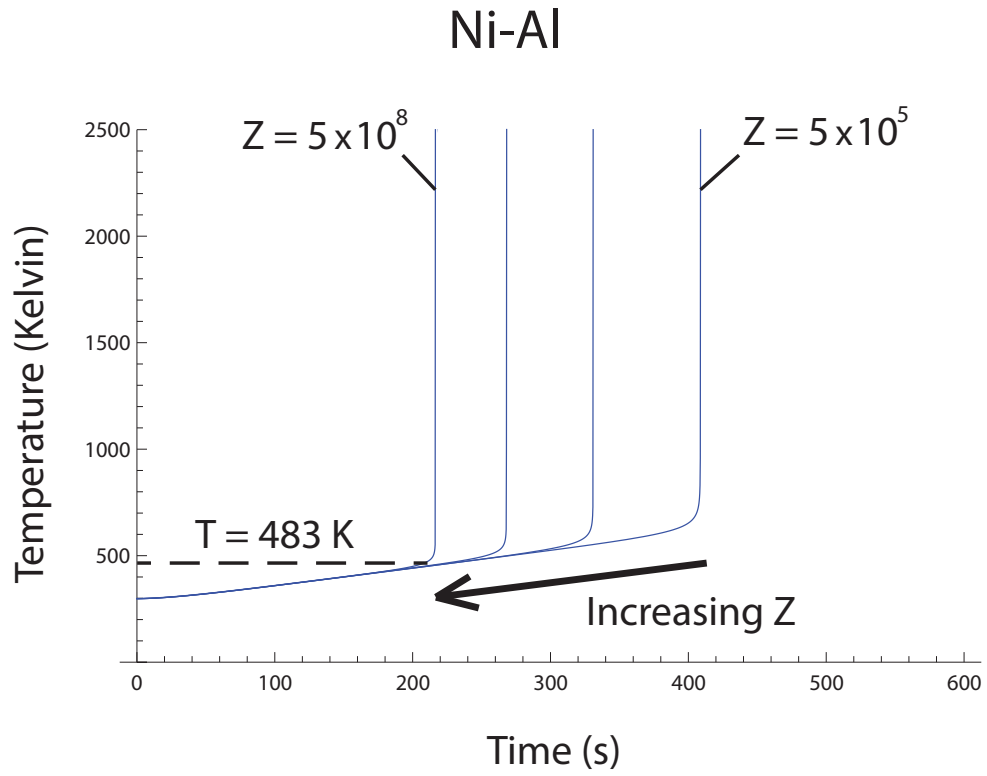


Figure 4.3: Ignition model for Ni-Al for varying values of pre-exponential factor Z

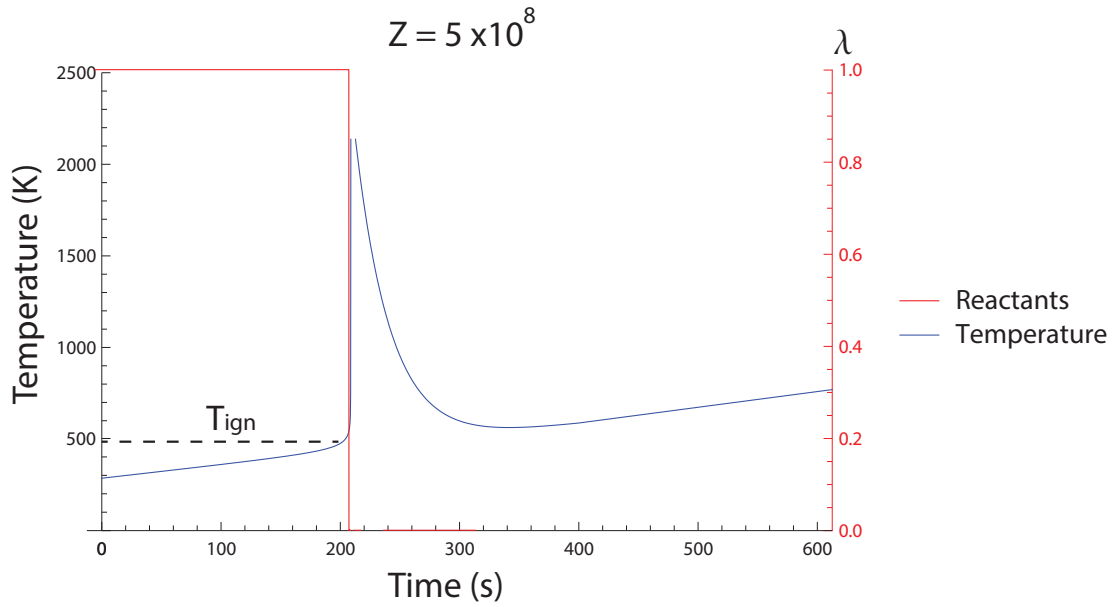


Figure 4.4: Temperature (blue) and concentration (red) evolution with time of Ni-Al from the ignition model

4.2 Two Phase Ignition Model

Similar to single phase reactions, lumped capacitance analysis is assumed for a two phase reaction model. The ODE system for a two phase hybrid system can be taken via the combination of two single phase reactions.

$$(m_1 C_{v1} + m_2 C_{v2}) \frac{dT}{dt} = m_1 Q_1 \lambda_1 \exp\left(-\frac{E_{a1}}{RT}\right) + m_2 Q_2 \lambda_2 \exp\left(-\frac{E_{a2}}{RT}\right) - hA(T - T_\infty) - \sigma \varepsilon A (T^4 - T_\infty^4) \quad (4.8)$$

$$\frac{d\lambda_1}{dt} = -Z_1 \lambda_1 \exp\left(-\frac{E_{a1}}{RT}\right) \quad (4.9)$$

$$\frac{d\lambda_2}{dt} = -Z_2 \lambda_2 \exp\left(-\frac{E_{a2}}{RT}\right) \quad (4.10)$$

$$\frac{dT_\infty}{dt} = K \quad (4.11)$$

Here, subscript 1 represents the Al-CuO terms, and subscript 2 represents the Ni-Al parameters. The term Q_i is the heat release of the respective compound, and T_∞ represents the ambient temperature of the system. Z_1 is the pre-exponential factor of Al-CuO (10^{14}), Z_2 is the pre-factor for Ni-Al ($5 \cdot 10^8$), and K is the heating rate. The thermo-chemical parameters used for individual compounds are found in table 4.1.

Figure 4.5 shows the temperature evolution of a hybrid system for varying concentrations of Ni-Al. For a case of 10% added Ni-Al, a small increase in temperature is observed at approximately 300 seconds. This increase shows that the Ni-Al in the hybrid mixture reacted, but the heat of reaction was not sufficient to ignite the entire mixture. The reaction of Al-CuO happens later at 873 K. Higher concentrations of added Ni-Al lead to an increase in this initial "bump" in temperature. Increasing the Ni-Al concentration also makes this increase in temperature happen sooner. Figure 4.6 shows the temperature and concentration evolution for a case of 22.15% Ni-Al mass fraction. At 255 seconds, the increase in temperature is observed, and we conclude that the Ni-Al completely reacts at this point. A small decrease in Al-CuO reactants (λ_1) shows that some Al-CuO also begins to react at this point.

Figure 4.7 shows the temperature evolution with respect to time for the hybrid ignition model, for concentrations of Ni-Al of 22.2% and greater. This figure shows the cases where ignition occurs at 500-480 K. These results show that for our model, the amount of added Ni-Al required to ignite the mixture is 22.2%. Higher concentrations of Ni-Al decrease the ignition temperature by small amounts. At 22.2% Ni-Al the ignition temperature is approximately 500 K, and at 75% Ni-Al the ignition temperature is approximately 480 K. Cases shown in figure 4.5 were assumed to have ignition temperatures of 873 K, and cases shown in figure 4.7 were assumed to have ignition temperatures of 480-500 K depending on the concentration of Ni-Al.

Figure 4.8 shows the temperature evolution of both the experimental data of a milled hybrid system and the modelled results with respect to time. The experimental data for a milled system shows that the decrease to lower temperatures occurs smoothly, and this transition happens at concentrations of 25% added Ni-Al. The model shows a more abrupt transition to lower ignition temperatures. This transition to lower ignition temperatures occurs at approximately 22.2% of added Ni-Al by mass.

Hybrid

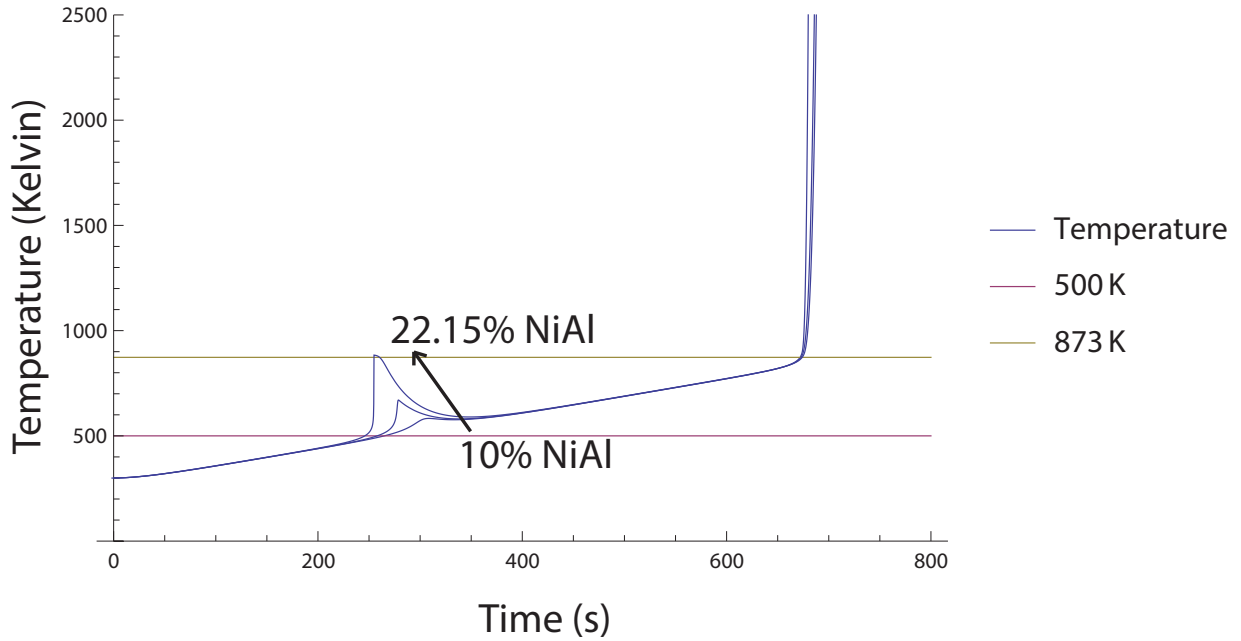


Figure 4.5: Typical temperature evolution for an ignition model of a hybrid system where the ignition temperature occurred at 873 K

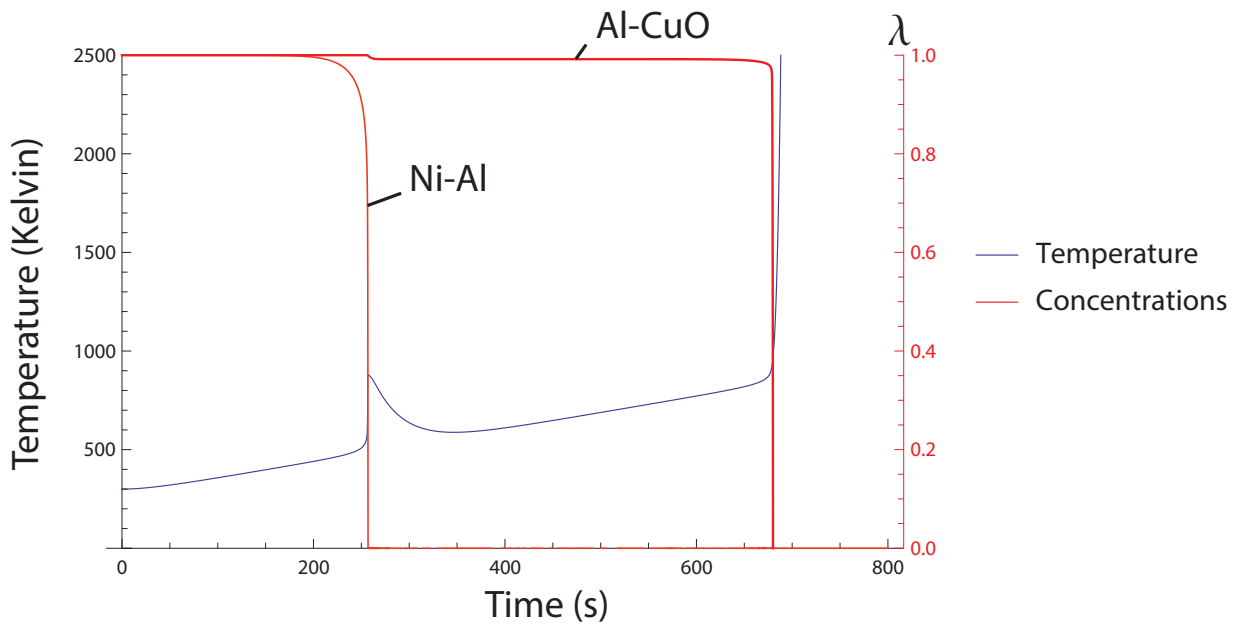


Figure 4.6: Ignition model showing the temperature (blue) and concentration (red) evolution of a hybrid mixture with 22.15% added Ni-Al

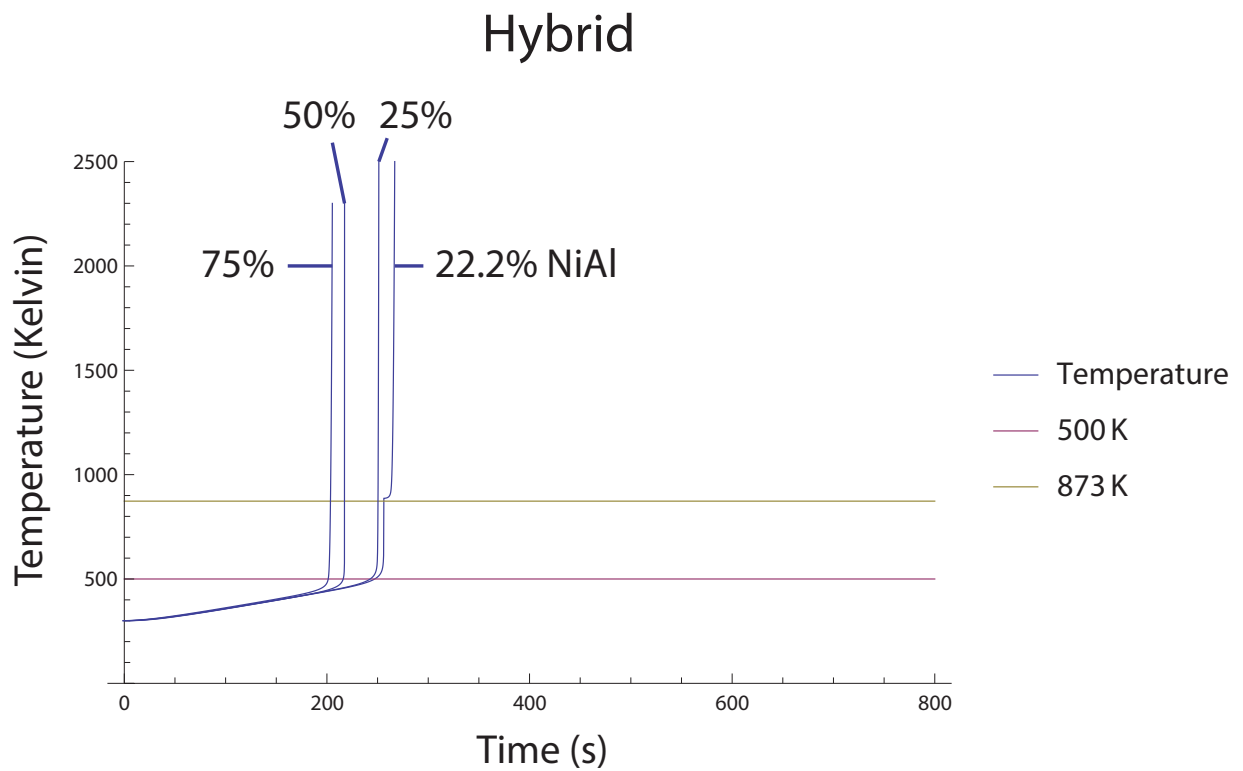


Figure 4.7: Typical temperature evolution for an ignition model of a hybrid system where the ignition temperature occurred at 500 K

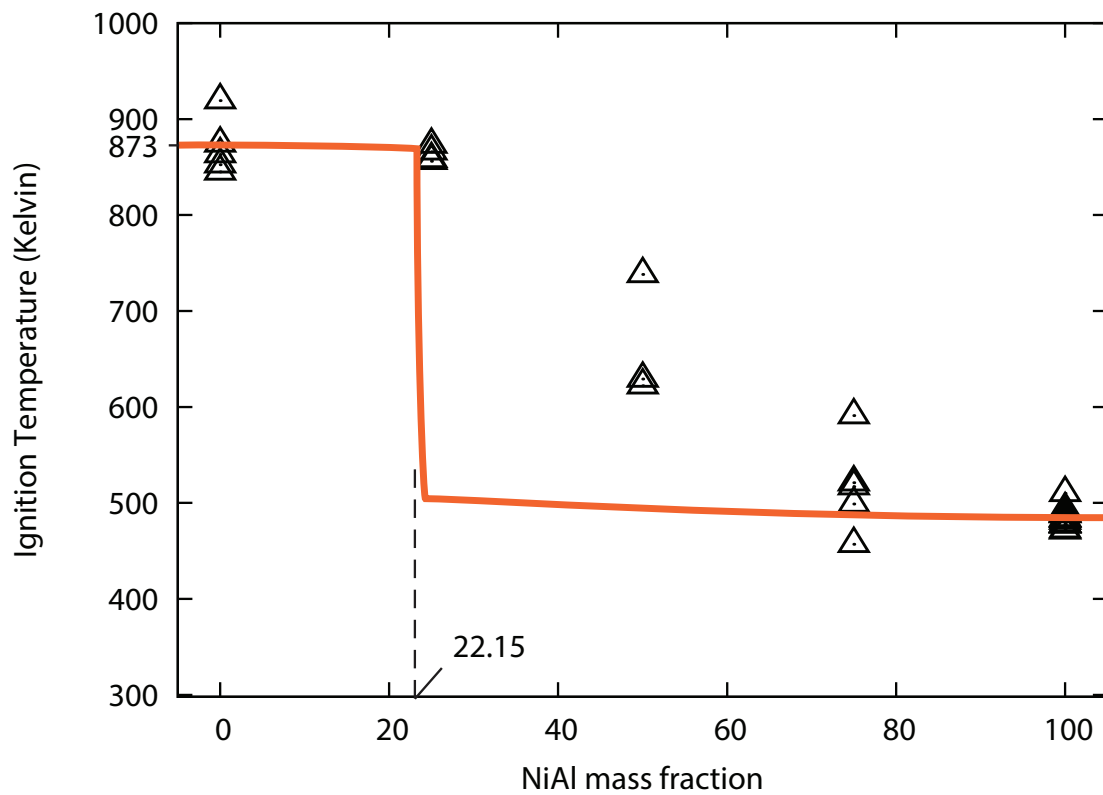


Figure 4.8: Experimental and theoretical temperature evolution with respect to the concentration of added Ni-Al in a hybrid system

Chapter 5

Further Discussions and Recommendations

5.1 Mechanical alloying

5.1.1 Al-CuO

Results have shown the effects of arrested reactive milling on the ignition temperatures of mixtures of Al-CuO. For a pure system of Al-CuO, the ignition temperatures were strongly dependent on the milling time. A 16 minute milled system had an ignition temperature of 873 K. For mill times of 30 and 46 minutes, ignition temperature results showed a transition in ignition temperatures. For the same mixture of milled powders, ignition temperatures are either 873, or 470-420 K. Milling times of 60 minutes and more yielded ignition temperatures of approximately 420 K, coinciding with the formation of intermediate phases. Umbrajkar et al. [7] have also shown lower ignition temperatures for longer periods of milling.

The selected range of heating rates for this study was relatively small, because the furnace did not have a high power output. Future work could be done with a furnace that has a higher heat output, which could lead to heating rates between 10^2 - 10^3 K/min.

Figure 3.3 shows the x-ray diffraction study results for unmilled and milled Al-CuO. A 16 minute milled system of Al-CuO yielded concentrations nearly identical to the raw Al-CuO powders. After 30 minutes of milling, secondary phases were present. These intermediate phases may explain the transitional behaviour of the milled powders. More work is needed in order to better understand the role of these secondary phases in the reaction kinetics of Al-CuO. Work could be done to observe the effects of the quantity of hexane on the results for the ignition temperatures, and phase concentrations.

5.1.2 Ni-Al

Mechanical alloying performed on mixtures of Ni-Al yielded more refined micro-structures, similar to what was shown by Mukasyan et al.[28]. In our study, production of nano-laminates was observed for all milling times. These nano-laminates improved the surface contact between constituents. A 40 minute milled Ni-Al mixture contained a very large quantity of these nano-laminates, which is believed to reduce the overall ignition temperature of the mixture and improve reaction kinetics. The constituent interface for a 40 minute milled system was reduced down to a nano-scale. The overall particle size of a 40 minute milled system remained consistent with the starting particle size which may vary between 5-25 μ m. Similar to Al-CuO, longer periods of milling resulted in lower ignition temperatures. A 16 minute milled system of Ni-Al had an average ignition temperature of approximately 625 K, and a 40 minute milled system had an ignition temperature of 480 K. It is believed that a decrease in constituent particle size, and an increase in surface contact ratio between constituents lead to the decrease in ignition temperatures. Figure 3.16 shows that ignition temperatures had a decreasing trend that was relatively linear when compared to Al-CuO results. XRD analysis concluded that no secondary phases were present. The lowered ignition temperatures can therefore be attributed solely to the refined micro-structure and improved contact surface between constituents. The work in this thesis confirmed what has been observed in previous studies [20, 28].

5.2 Hybrid System

An unmilled hybrid system was created using 16 minute milled Al-CuO and 40 minute milled Ni-Al. Figure 3.19 shows that mixtures of 25% and 50% added Ni-Al by mass reacted at 873 K. It was only at 65% and 75% that a decrease was observed. A transitional behaviour was observed in the ignition temperatures of a hand mixed Al-CuO-Ni system, similar to what was observed for 30 and 46 minute milled Al-CuO systems. This may be attributed to the fact that pellets were not homogeneous, and the concentrations of Ni-Al would vary locally. Some pellets might have had enough Ni-Al locally, which would create enough heat to initiate the reaction. Ultra-sonic mixing could have been implemented for the mixing of 40 minute Ni-Al and 16 minute Al-CuO, in order to have better particle distribution inside the hybrid mixture. Better distribution could lead to more consistent ignition temperature results.

A milled hybrid system was studied to see the effects of an improved particle distribution. Results shown in figure 3.25 demonstrate that a milled hybrid system has ignition temperatures decreasing gradually with concentration of Ni-Al. This smoother trend may be attributed to the fact that nickel particles are now evenly distributed due to ARM. The heat generated by the Ni-Al reaction would now be evenly distributed throughout the sample. In future work, the heat generated by these new hybrid mixtures could be analysed using differential scanning calorimetry. It would be important to note how the exothermicity of an Al-CuO-Ni system compares with a 30 minute milled Al-CuO system that had secondary phases present. In future studies, flame propagation speed measurements should be conducted to quantify the influence of concentration of Ni-Al on a hybrid mixture of Al-CuO-Ni.

The proposed ignition model captured the behaviour of individual compounds. However, for the two phase hybrid model the transition to lower ignition temperatures was much more abrupt, and occurred at lower concentrations of added Ni-Al compared to what was captured in the experiments. Improvements on this ignition model could be made to better capture the experimental behaviour of these hybrid mixtures, as well as considering the heterogeneous effects.

Chapter 6

Conclusion

The ARM method has proved to be successful in reducing the ignition temperatures of thermites and intermetallic compounds. Products and intermediate phases formed for mixtures of Al-CuO that were milled for more than 16 minutes. Due to product formation during milling, the ARM method alone was not a viable option to lower the ignition temperature of Al-CuO. The lowest ignition temperature obtained for Al-CuO without formation of intermediate phases using ARM, was for a 16 minutes milled system. This mixture had an average ignition temperature of 600°C. Milling of nickel-aluminium yielded significantly lower ignition temperatures averaging 210°C for 40 minute milled samples. The addition of this milled intermetallic mixture to Al-CuO reduced the ignition temperature of both milled and unmilled hybrid systems. The milled system had lowered ignition temperatures for concentrations of Ni-Al more than 50%. Concentrations of 75% Ni-Al had ignition temperatures of approximately 250°C. The unmilled Hybrid mixture had ignition temperatures of 600°C for concentrations of 25% and 50% Ni-Al. A sharp decrease in ignition temperatures was observed for concentrations of 65% and 75%. The lowest ignition temperature observed was 200°C for the milled hybrid system at concentrations of 75% Ni-Al. This mixture answers our objectives as it had low ignition temperatures, and had no intermediate phases. Milling a hybrid mixture is easily scalable which makes this method attractive for commercial applications.

Appendices

Appendix A

Mathematica Code for Ignition Model

```
ClearAll
```

```
ClearAll
```

Note that items 1 refer to Al-CuO
items 2 refer to Ni-Al

```
In[50]:=
```

```
Ea1 := 277000.
```

```
Ea2 := 104000.
```

```
R := 8.314
```

```
Cv1 := 0.653
```

```
Cv2 := 0.588
```

```
h := 20.
```

```
Q1 := 4077.
```

```
Q2 := 1300.
```

```
Z1 := 50000000000000.
```

```
Z2 := 50000000.
```

```
A := 3.53 * (10^-5)
```

```
m1 := (0.0356) * 0
```

```
m2 := (0.0356) * 1
```

```
In[63]:= eqns = {
```

$$m1 * Cv1 * D[T[t], t] + m2 * Cv2 * D[T[t], t] == m1 * Z1 * Q1 * \lambda_1[t] * \text{Exp}\left[\frac{-Ea1}{R * T[t]}\right] +$$

$$m2 * Z2 * Q2 * \lambda_2[t] * \text{Exp}\left[\frac{-Ea2}{R * T[t]}\right] - h * A * (T[t] - \alpha[t]),$$

$$D[\lambda_1[t], t] == -Z_1 * \lambda_1[t] * \text{Exp}\left[\frac{-E_{a1}}{R * T[t]}\right],$$

$$D[\lambda_2[t], t] == -Z_2 * \lambda_2[t] * \text{Exp}\left[\frac{-E_{a2}}{R * T[t]}\right],$$

$$D[\alpha[t], t] == 0.83,$$

$$T[0] == 300,$$

$$\alpha[0] == 300,$$

$$\lambda_1[0] == 1,$$

$$\lambda_2[0] == 1\}$$

```
In[66]:= sol = NDSolve[eqns, {T[t], λ1[t], λ2[t]}, {t, 0, 700}]
```

```
In[67]:= p11 = Plot[{T[t] /. sol, 500}, {t, 0, 800},  
PlotRange -> {300, 1500}, AxesLabel -> {time (s), Temperature},  
PlotLegends -> {Temp. Evolution, 500 Kelvin, 863 K}]
```

References

- [1] S. H. Fischer and M. Grubelich, “Theoretical energy release of thermites, intermetallics, and combustible metals,” tech. rep., Sandia National Labs., Albuquerque, NM (US), 1998.
- [2] K. K. Kuo, G. A. Risha, B. J. Evans, and E. Boyer, “Potential usage of energetic nano-sized powders for combustion and rocket propulsion,” in *MRS Proceedings*, vol. 800, pp. AA1–1, Cambridge Univ Press, 2003.
- [3] E. L. Dreizin, “Metal-based reactive nanomaterials,” *Progress in Energy and Combustion Science*, vol. 35, no. 2, pp. 141–167, 2009.
- [4] T. W. LTD, “Thermit welding process,” 2014.
- [5] J. Agrawal, “Recent trends in high-energy materials,” *Progress in energy and combustion science*, vol. 24, no. 1, pp. 1–30, 1998.
- [6] P. F. Pagoria, G. S. Lee, A. R. Mitchell, and R. D. Schmidt, “A review of energetic materials synthesis,” *Thermochimica Acta*, vol. 384, no. 1, pp. 187–204, 2002.
- [7] S. M. Umbrajkar, M. Schoenitz, and E. L. Dreizin, “Exothermic reactions in al-cuo nanocomposites,” *Thermochimica acta*, vol. 451, no. 1, pp. 34–43, 2006.
- [8] O. M. Y. C.-T. J. L. A. Bacciochini, M. Radulescu, “Enhanced reactivity of mechanically-activated nano-scale gasless reactive materials consolidated via the cold-spray technique,” in *APS Shock Compression of Condensed Matter Meeting Abstracts*, vol. 1, p. 2003, 2011.

- [9] S. G. F.D. Tang, A.J. Higgins, “Effect of discreteness on heterogeneous flames: propagation limits in regular and random particle arrays,” *Combustion Theory and Modelling*, vol. 13, no. 2, pp. 319–341, 2009.
- [10] E. M. Hunt and M. L. Pantoya, “Ignition dynamics and activation energies of metallic thermites: From nano-to micron-scale particulate composites,” *Journal of applied physics*, vol. 98, no. 3, p. 034909, 2005.
- [11] A. D. Kirshenbaum, “Effect of different carbons on ignition temperature and activation energy of black powder,” *Thermochimica Acta*, vol. 18, no. 1, pp. 113–123, 1977.
- [12] V. Y. Zelinskii, N. Yavorovskii, L. Proskurovskaya, and V. Davydovich, “Structural state of aluminum particles prepared by electric explosion,” *Fizika i Khimiya Obrabotki Materialov*, vol. 1, pp. 57–59, 1984.
- [13] H. Calcote and W. Felder, “A new gas-phase combustion synthesis process for pure metals, alloys, and ceramics,” in *Symposium (International) on Combustion*, vol. 24, pp. 1869–1876, Elsevier, 1992.
- [14] K. T. Higa, R. A. Hollins, and C. E. Johnson, “Preparation of fine aluminum powders by solution methods,” Mar. 23 1999. US Patent 5,885,321.
- [15] V. Chawla, S. Prakash, and B. Sidhu, “State of the art: Applications of mechanically alloyed nanomaterials a review,” *Materials and Manufacturing processes*, vol. 22, no. 4, pp. 469–473, 2007.
- [16] J. Benjamin and T. Volin, “The mechanism of mechanical alloying,” *Metallurgical Transactions*, vol. 5, no. 8, pp. 1929–1934, 1974.
- [17] C. Suryanarayana, “Mechanical alloying and milling,” *Progress in materials science*, vol. 46, no. 1, pp. 1–184, 2001.
- [18] S. M. Umbrajkar, M. Schoenitz, and E. L. Dreizin, “Control of structural refinement and composition in al-moo₃ nanocomposites prepared by arrested reactive milling,” *Propellants, Explosives, Pyrotechnics*, vol. 31, no. 5, pp. 382–389, 2006.

- [19] J. Keskinen, A. Pogany, J. Rubin, and P. Ruuskanen, "Carbide and hydride formation during mechanical alloying of titanium and aluminium with hexane," *Materials Science and Engineering: A*, vol. 196, no. 1, pp. 205–211, 1995.
- [20] K. V. Manukyan, B. A. Mason, L. J. Groven, Y.-C. Lin, M. Cherukara, S. F. Son, A. Strachan, and A. S. Mukasyan, "Tailored reactivity of ni+al nanocomposites: Microstructural correlations," *Journal of Physical Chemistry C*, vol. 116, pp. 21027–21038, 2012.
- [21] A. Ermoline, D. Stamatis, and E. Dreizin, "Low-temperature exothermic reactions in fully dense al–cuo nanocomposite powders," *Thermochimica Acta*, vol. 527, pp. 52–58, 2012.
- [22] D. Stamatis, Z. Jiang, V. K. Hoffmann, M. Schoenitz, and E. L. Dreizin, "Fully dense, aluminum-rich al-cuo nanocomposite powders for energetic formulations," *Combustion Science and Technology*, vol. 181, no. 1, pp. 97–116, 2008.
- [23] J. J. Granier and M. L. Pantoya, "Laser ignition of nanocomposite thermites," *Combustion and Flame*, vol. 138, no. 4, pp. 373–383, 2004.
- [24] K. Ilunga, O. Del Fabbro, L. Yapi, and W. W. Focke, "The effect of si₂-bi₃ on the ignition of the al-cuo thermite," *Powder Technology*, vol. 205, no. 1, pp. 97–102, 2011.
- [25] Y. L. Shoshin, M. A. Trunov, X. Zhu, M. Schoenitz, and E. L. Dreizin, "Ignition of aluminum-rich al-ti mechanical alloys in air," *Combustion and flame*, vol. 144, no. 4, pp. 688–697, 2006.
- [26] M. Schoenitz, S. M. Umbrajkar, and E. L. Dreizin, "Kinetic analysis of thermite reactions in al-moo₃ nanocomposites," *Journal of Propulsion and Power*, vol. 23, no. 4, pp. 683–687, 2007.
- [27] E. Bahrami Motlagh, J. Vahdati Khaki, and M. Haddad Sabzevar, "Welding of aluminum alloys through thermite like reactions in al–cuo–ni system," *Materials Chemistry and Physics*, vol. 133, no. 2, pp. 757–763, 2012.

- [28] A. Mukasyan, J. White, D. Y. Kovalev, N. Kochetov, V. Ponomarev, and S. Son, “Dynamics of phase transformation during thermal explosion in the al–ni system: Influence of mechanical activation,” *Physica B: Condensed Matter*, vol. 405, no. 2, pp. 778–784, 2010.
- [29] A. Bacciochini, M. Radulescu, Y. Charron-Tousignant, J. Van Dyke, M. Nganbe, M. Yandouzi, J. Lee, and B. Jodoin, “Enhanced reactivity of mechanically-activated nano-scale gasless reactive materials consolidated by coldspray,” *Surface and Coatings Technology*, vol. 206, no. 21, pp. 4343–4348, 2012.
- [30] G. Maines, M. I. Radulescu, A. Bacciochini, B. Jodoin, and J. Lee, “Pressure waves generated by metastable intermolecular composites in an aqueous environment,” in *Bulletin of the American Physical Society. 18th Biennial Intl. Conference of the APS Topical Group on Shock Compression of Condensed Matter held in conjunction with the 24th Biennial Intl. Conference of the Intl. Association for the Advancement of High Pressure Science and Technology (AIRAPT); Seattle, Washington.,* vol. 58, 7-12 July 2013.
- [31] J. Holman, *Heat Transfer 10th edition*. Raghathan Srinivasan, 2010.
- [32] H. Akbarnejad, “Influence of porosity on the flame speed in gasless biometric reactive systems,” Master’s thesis, University of Ottawa, 2013.
- [33] G. M. Fritz, *Characterizing the Ignition Threshold of Multilayer Reactive Materials and Controlling Reaction Velocities in Compacts of Reactive Laminate Particles*. PhD thesis, Johns Hopkins University, 2011.
- [34] J. Sun, M. L. Pantoya, and S. L. Simon, “Dependence of size and size distribution on reactivity of aluminum nanoparticles in reactions with oxygen and moo_3 ,” *Thermochimica Acta*, vol. 444, no. 2, pp. 117–127, 2006.
- [35] A. S. Shteinberg, Y.-C. Lin, S. F. Son, and A. S. Mukasyan, “Kinetics of high temperature reaction in ni-al system: influence of mechanical activation,” *The Journal of Physical Chemistry A*, vol. 114, no. 20, pp. 6111–6116, 2010.

[36] O. Engineering, "Emissivity of common materials."